Beatriz Jorge Coelho

Licenciatura em Ciências de Engenharia de Micro e Nanotecnologias

A Digital Microfluidics Platform for Loop-Mediated Isothermal Amplification of DNA

Dissertação para obtenção do Grau de Mestre em Engenharia de Micro e Nanotecnologias

Orientador: Professor Doutor Rui Alberto Garção Barreira do Nascimento Igreja, Departamento de Ciências dos Materiais, Faculdade de Ciências e Tecnologia – Universidade Nova de Lisboa

Co-orientador: Professor Doutor Pedro Viana Baptista, Departamento de Ciências da Vida, Faculdade de Ciências e Tecnologia – Universidade Nova de Lisboa

Júri

Presidente: Professor Doutor Rodrigo Ferrão de Paiva Martins

Arguente: Professor Doutor José Ricardo Ramos Franco Tavares

Vogal: Professor Doutor Rui Alberto Garção Barreira do Nascimento Igreja

FACULDADE DE CIÊNCIAS E TECNOLOGIA
UNIVERSIDADE NOVA DE LISBOA

September 2016

A Digital Microfluidics Platform for Loop-Mediated Isothermal Amplification of DNA

© Beatriz Jorge Coelho

Faculdade de Ciências e Tecnologia

Universidade Nova de Lisboa

Acknowledgements

This thesis marks the end of one of the most important steps in my life: university. However, it also marks the beginning of my future as a professional worker. As Lucius Annaeus Seneca would say, somewhere around the first Christian decades, *every new beginning comes from other beginning's end.* This new beginning would have never been possible without the precious assistance of many people, which is why the first page of this thesis is entirely dedicated to them.

First of all, I would like to thank Professor Rodrigo Martins and Professor Elvira Fortunato, for bringing my course to life and for taking Portuguese Nanotechnology to the highest level in the world. The work you have developed over the past years, as well as the worldwide acknowledgement that you have achieved, were two of the reasons that motivated me to choose Micro and Nanotechnology Engineering.

Secondly, to my parents, who are truly responsible for who I am and what I have achieved. Their endless patience and willingness to help in everything they could was a key factor to the completion of this manuscript. Thank you for always being there, in all the happy and sad moments, whether I was gleefully cheerful or with an unprecedented bad mood. Thirdly, I would like to thank those who are carelessly and repeatedly forgotten, even though they are the most loyal and faithful of friends. To my dogs, Aquiles and Bianca, thank you for always receiving me with so much joy whenever I get home, whether rain is pouring or the sun is shining.

Then, to my closest friends, Eunice Beijinho, Cláudio Brito, Priscila Deister and Helena Gaspar thank you so much for always being around for the past 17, or even 23 (!) years. You may be short in numbers, but believe me when I tell you that you are truly 4 in 7.4 billion people.

And, of course, there is also a very long list of people to thank in the four institutions that were my home for the past months: CENIMAT, CEMOP, Department of Life Sciences (DCV) and Department of Materials Science (DCM).

Beginning with the physics/materials half of my academic life, special thanks are in order to Inês Cunha, for all her advice and support, to Andreia Santos, for being my ever patient official care-taker and also to Tiago Carvalho, the first adviser I ever had. I would also like to thank Paul Grey, Raquel Barras, and Pedro Freitas for their eternal good mood and for waiting for me at lunch time. I mustn't forget thanking the "background people", who are not directly involved with my work and yet are fundamental to its success: Lídia Ricardo, Ana Santa, Carolina Marques, Alexandra Gonçalves and Sónia Pereira.

As for the biology part of my work, I would like to thank Fábio Carlos, Pedro Pedrosa, Mílton Cordeiro and Raquel Vinhas for being always available to enlighten me about anything, and for maintaining their poise even while being fiercely attacked by thousands of questions. You're all absolutely brilliant. I would also like to thank my colleagues and friends from the 315 laboratory: Ana Sofia Matias, Cindy Oliveira and Ana Rita Mendes. To Sofia, thank you so much for teaching me how to spell my first biological procedures and how to count with pipette tips and microtubes. To Cindy, thank you for being my wingman(woman) when I was busy dividing myself between both edges of the campus, and thank you for your great sense of humor and terrible taste in music. To Rita, thank you for brightening my day with your contagious wit, and for our great, smiley chats about the not-so-great parts of our work. Also, thank you, António Lopez, for helping me catch the train more often, and for all your optimistic kindness.

And, of course, last but not least, I would like to thank the hybrid (or should I say, high breed?) Bruno Veigas for all the Snape-like harangues and preposition-ending sentences which taught me how to think, criticize and act (almost) like a full-fledged researcher.

Moreover, I would like to thank both my supervisors, Professor Rui Igreja and Professor Pedro Baptista, for their precious guidance throughout my work, and for bearing with my stubbornness.

I would also like to thank Professor Hugo Águas, for his precious tips on photolithography, and for allowing me to work at the DCM clean room.

Also, to my colleagues from the best course in the entire world, thank you so much for making the last 5 years the most memorable years of my life. Thank you for teaching me how to work as a team and for showing me the importance of helping others, both inside and outside our work group. In particular, I would like to thank Joana Cerdeira, for her optimism, and for having the highest percentage of strength per kg. To Mónica Machado, thank you for bringing such high doses of laughter to my life. I will always remember your funniest moments! Trust yourself a bit harder, and you will go far. Thank you both for endless chit-chats during lunch time! I would also like to thank Miguel Franco for your brilliant, wonderful dark humour. Your gloomful, black star always shines over my pink world. Bring the hammer, Miguel!

Abstract

Digital Microfluidics (DMF) is an innovative technology for liquid manipulation at microliter- to picoliter-scale, with tremendous potential of application in biosensing. DMF allows maneuvering single droplets over an electrode array, by means of electrowetting-on-dielectric (EWOD), that allows changing the contact angle of a droplet over a dielectric. Each droplet is thus considered a microreactor, with an unparalleled potential to perform chemical and biological reactions. Several aspects inherent to DMF platforms, such as multiplex assay capability and integration capability, make them promising for lab-on-chip and point-of-care (PoC) applications, *e.g.* DNA amplification assays or disease detection. DNA detection strategies for PoC have been profiting from recent development of isothermal amplification schemes, of which Loop-mediated Isothermal Amplification (LAMP) is a major methodology, allowing a 10^9-fold amplification efficiency in one hour.

Here, I demonstrate for the first time the effective coupling of DMF and LAMP, resulting in a DMF device capable of performing LAMP reactions.

This novel DMF platform has been developed and characterised, which allows successful amplification of a *c-Myc* gene fragment by LAMP. Precise temperature control is achieved by using a transparent heating element, connected to a looping feedback control system. This platform is able to amplify just 0.5 ng/µL of the target DNA, in only 45 minutes, for a device temperature of 65 °C and a reaction volume of 1.62 µL, one of the lowest volumes ever reported. Moreover, the electrophoretic analysis indicates that the amplification efficiency of the on-chip LAMP is considerably higher than that from the bench-top reaction.

Keywords: Digital Microfluidics, Loop-mediated Isothermal Amplification, *c-Myc*, lab-on-chip, point-of-care diagnostics.

Resumo

A Microfluídica Digital (MFD) é uma tecnologia inovadora que permite manipular líquidos à escala dos microlitros a picolitros, apresentando um tremendo potencial de aplicação em biossensores. A MFD permite manobrar gotas individuais sobre uma matriz de elétrodos, através do fenómeno *electrowetting-on-dielectric* (EWOD), que por sua vez permite a alteração do ângulo de contacto de uma gota sobre um material dielétrico. Cada gota pode então ser considerada um microreator, com um potencial extraordinário para realizar reações químicas e biológicas. Vários aspetos inerentes a plataformas de MFD, tais como a sua capacidade para ensaios multiplex ou a sua capacidade de integração, tornam-nas bastante promissoras para aplicações *lab-on-chip* e *point-of-care* (PoC), p.e. ensaios de amplificação de DNA e deteção de doenças. As estratégias de deteção de DNA para PoC têm beneficiado do desenvolvimento recente de técnicas de amplificação isotérmica, das quais a *Loop-mediated Isothermal Amplification* (LAMP) é uma das principais metodologias, permitindo uma eficiência de amplificação de 10^9 vezes em apenas uma hora.

Aqui, demonstro pela primeira vez a integração/acoplamento de MFD e LAMP, o que resultou num dispositivo de MFD capaz de realizar reações de LAMP.

Esta nova plataforma de MFD foi desenvolvida e caracterizada neste trabalho, e permite a amplificação de um fragmento do gene *c-Myc* por LAMP, com sucesso. É possível garantir um controlo de temperatura bastante preciso, através de um elemento de aquecimento transparente ligado a um sistema de controlo com retroalimentação. Esta plataforma permite amplificar apenas 0.5 ng/µL do DNA alvo, em 45 minutos, para uma temperatura do dispositivo de 65 °C e um volume de reação de 1.62 µL, um dos volumes mais baixos alguma vez descritos. Para além do mais, a análise eletroforética indica que a eficiência de amplificação de LAMP no dispositivo é consideravelmente superior àquela de uma reação de bancada.

Termos chave: Microfluídica Digital, *Loop-mediated Isothermal Amplification*, *c-Myc*, *lab-on-chip*, *point-of-care diagnostics*.

Contents

List of figures

List of tables

List of abbreviations

µLAMP	Micro-Loop-mediated isothermal amplification
AC	Alternating current
BIP	Backward inner primer
Bp	Base pair
CEMOP	Centro de Excelência de Optoeletrónica e Microeletrónica de Processos
CENIMAT	Centro de Investigação de Materiais
CT	Threshold cycle
CVD	Chemical vapour deposition
DC	Direct current
DCM	Departamento de Ciências dos Materiais
DCV	Departamento de Ciências da Vida
DMF	Digital Microfluidics
DNA	Deoxyribonucleic acid
E-coli	*Escherichia coli*
EDL	Electric double layer
EWOD	Electrowetting-on-dielectric
FIP	Forward inner primer
GPIB	General purpose interface bus
ITO	Indium-Tin-Oxide
LAMP	Loop-mediated isothermal amplification
LB medium	Luria-Bertani medium
LOD	Limit of detection
MRSA	Methicillin-resistant *Staphylococcus aureus*
NASBA	Nucleic acid sequence-based amplification
PCB	Printed circuit boards
PCR	Polymerase Chain Reaction
PDMS	Polydimethylsiloxane
PID	Proportional-integral-derivative
PoC	Point-of-care
PWM	Pulse width modulation
RMS	Root mean square
RNA	Ribonucleic acid
SAW	Surface acoustic waves
SDA	Strand displacement amplification
SMART	Signal mediated amplification of RNA technology
USD	United States Dollar
UV	Ultraviolet

List of symbols

C	Capacitance
C^*	Complex capacitance
C'	Real part of the capacitance
C''	Imaginary part of the capacitance
d	Distance between capacitor plates
R	Resistance
Rs	Series resistance
T	Temperature
$\tan(\delta)$	Loss tangent
V	Voltage
Z	Impedance
γ	Surface tension
γ_{LG}	Liquid-gas surface tension
ε_0	Permittivity in vacuum (8.85×10^{-12} Fm^{-1})
ε_r	Relative permittivity, dielectric constant
θ	Contact angle
θ_0	Non-actuated contact angle

Motivation and Objectives

Digital Microfluidics (DMF) is a versatile and innovative technique for fluid manipulation, which relies on an electrode array to produce electric fields capable of moving picoliter to microliter droplets. Since 2000, this liquid-handling approach has gathered increasing interest from the scientific community, resulting in a wide range of applications, mostly directed to the fields of chemistry, medicine and biotechnology. Immunoassays, chemical synthesis or proteomic procedures performed in droplet microreactors are just some of the possibilities enabled by DMF devices[1,2]. As a matter of fact, due to their ease of operation, flexibility, multiplex assay capability, as well as growing portability and integration capability, DMF platforms are considered promising candidates for lab-on-chip or even point-of-care applications[1,3,4].

Particularly, point-of-care diagnostics have met an enormous increase in demand over the past years, due to a series of factors which include prevalence of diseases in developing countries, rising incidence of lifestyle diseases such as diabetes or a significant trend towards healthcare decentralisation[5]. It is estimated that the point-of-care diagnostics market will reach a value of approximately 37 billion USD in 2021[6]. Part of point-of-care diagnostics include genetic testing, which is particularly relevant in oncology, pharmacogenomics and genetic diseases, three major health areas. As would be expected, this is a high value market, estimated to be worth 7.4 billion USD in 2020[7].

One of the most important tools in genetic testing is nucleic acid amplification, which relies greatly in Polymerase Chain Reaction (PCR) that is today the gold standard for DNA analysis. However, PCR requires thermal cycling with 3 different temperatures that add complexity to the technique. As such, isothermal nucleic acid amplification methods have been developed in the last decade, with emphasis to Loop-mediated Isothermal Amplification (LAMP).

Having in mind the current need for genetic testing, and considering that there are no publications describing a digital microfluidics platform for nucleic acid amplification based on LAMP, the main purpose of this work is to successfully implement this technique in such a device. This novel chip consists of a two-plate configuration on glass substrate, where the bottom plate includes: 1) a Parylene C dielectric layer; 2) a Teflon® hydrophobic layer and 3) chromium electrodes/reservoirs. The top plate consists of an Indium-Tin-Oxide (ITO) coated glass substrate, which also includes a hydrophobic Teflon® layer and drilled ports partially overlapping the reservoirs for sample/reagent inlet/outlet, by means of a pipette. These ports are also key features of the device, assuring a simpler, easier way to insert and withdraw samples. The gap between bottom and top plates is assured by Kapton® tape. Under the bottom plate, there is an ITO thin film thermoresistor, deposited on a glass substrate, which will provide the required temperature for LAMP reactions. More specifically, this DMF device is divided into four key regions: two main reservoirs to accommodate the target DNA and LAMP reagents, a mixing region where both sample and reagents are mixed and the reaction occurs, and finally another reservoir for product collection, all linked together by 4-electrode paths. The electrodes were produced in two configurations: a standard square electrode configuration, and a novel zig-zag electrode configuration.

Both reservoirs and electrodes are patterned by conventional photolithography, Parylene C is deposited by a specific Chemical Vapour Deposition (CVD) process and Teflon® is deposited by spin-coating. As for the target DNA sequence, a fraction of the *c-Myc* proto-oncogene was chosen, since the overexpression of this particular gene is associated with a large portion of all human cancers[8,9].

In order to achieve the main objective, the following tasks were performed:

- Extraction of target DNA;
- Practical study of both PCR and LAMP reactions;

- LAMP optimisation, for further integration in the DMF platform;
- Mask design for photolithography;
- Optimisation of the photolithographic process, namely Ultraviolet (UV)-light exposure, revelation process and lift-off;
- Device fabrication;
- Preliminary device testing;
- On-chip DNA amplification by LAMP.

1. Introduction

1.1. Digital Microfluidics

Digital Microfluidics is a relatively recent process for microflow control, based on microfluidics. In conventional microfluidics, fluids are constrained to micro-volume spaces and can therefore be controlled and manipulated with very high precision. The use of microfluidic devices versus macrofluidics allows several improvements: both sample and reagent volumes are significantly reduced, the final results or products are obtained in a shorter time, the sensitivity of the processes is increased and the risks associated with toxic reagents or products are decreased[10,11]. Additionally, portability and process automation due to miniaturisation are also key advantages for the processes' industrialisation[10].

Particularly, DMF is a relatively recent technology for liquid manipulation, which allows the control of discrete picoliter to microliter droplets in integrated systems, by means of electric potentials[1,12], magnetic[13], thermocapillary[14] or optic[15,16] forces, and even surface acoustic waves[17] (SAW). In addition to the above-mentioned advantages of microfluidic systems, DMF systems eliminate the need for using propulsion devices, such as valves or pumps and allow the precise control of individual unit-sized droplets via pre-established digital control commands[1]. As a direct consequence of individual droplet control, each droplet may be considered as a microreactor, which in turn allows the mixing of several reagents. Moreover, this technique is perfectly compatible with solid/liquid samples, allowing clogging-free separation of both phases[12]. There is also no need to change the platform design for different reactions, since DMF devices are often generic and any desired sequence of fluidic operations is possible.

The first literature reference to this type of process dates back to 1986, when Jean Pesant, Michael Hareng, Bruno Mourey and Jean Perbet submitted a patent describing a device *by means of which it is possible to cause fluid globules to circulate within a capillary space by means of pairs of electrodes establishing capture sites*[18]. Later, in the 2000s, DMF studies were continued by two American groups, namely the Fair[19] group at Duke University and the Kim[20] group at University of California, Los Angeles, which disseminated the technique.

1.1.1. Digital Microfluidics configurations

DMF devices are composed of four elements: substrate, electrodes, a dielectric layer and a hydrophobic layer. Additionally, the droplets may be surrounded by air, or by a filler, to improve actuation. These elements may be arranged in two main configurations: 1) the closed format (or two-plate format), in which droplets are sandwiched between two substrates and 2) the open format (or one-plate format), in which droplets move on a single substrate[12]. For the first configuration, the top plate is usually a ground electrode made of a transparent, conductive material, thus allowing the user to observe the movement of the droplets and even confirm that certain reactions have occurred (*e.g*, via colour change). The bottom plate allocates the actuation electrodes, which will allow the user to control the droplet path. As for the second configuration, the bottom plate includes the ground electrode, as well as the actuation electrodes[12]. In any case, the bottom plate is generally covered by an insulating dielectric. Finally, in order to enhance the electrowetting effect, a hydrophobic layer is applied to their surfaces. Both formats permit the moving and merging of droplets, but only the two-plate format enables splitting and dispensing operations[1,21]. Figure 1.1 shows the two structures available (a), as well as the various fluidic operations possible on DMF (b).

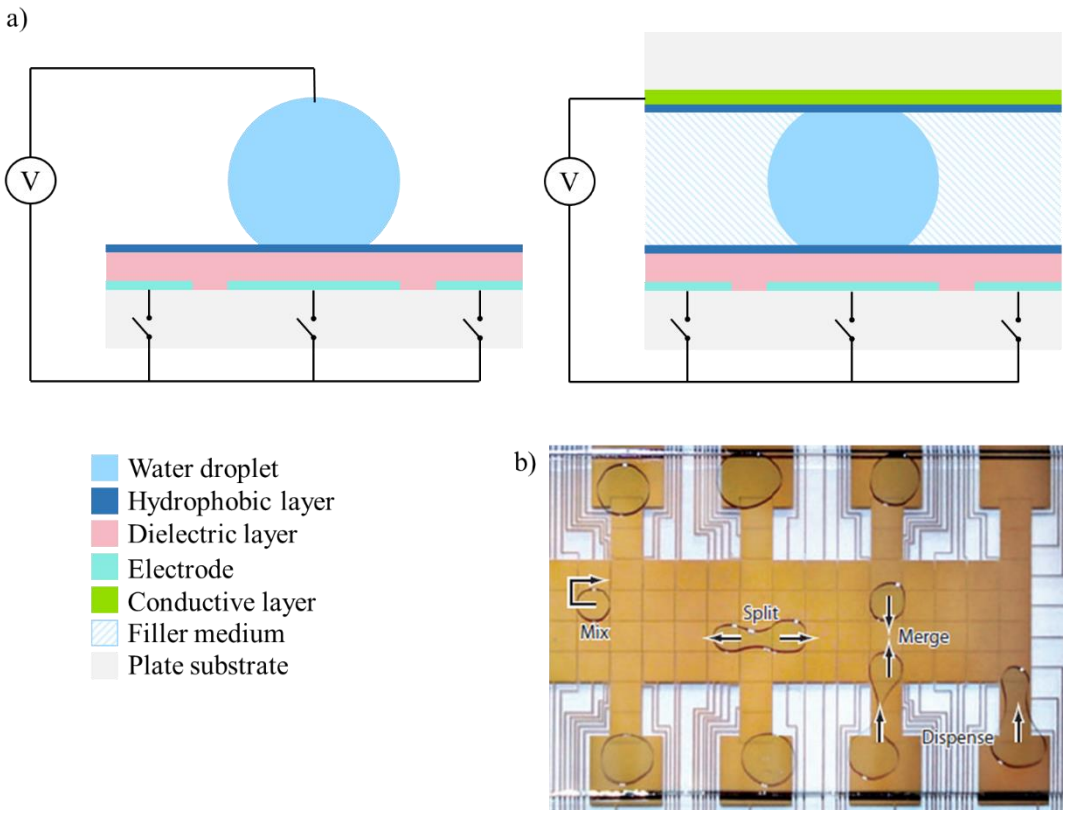

Figure 1.1: a) One-plate (left) and two-plate (right) configurations for DMF devices (not to scale); b) fluidic operations for a two-plate configuration: splitting, merging, mixing and dispensing (the latter was adapted from reference 1).

The proper choice of component materials is of key relevance in DMF, since it determines the fabrication process, as well as the possible geometries. Substrates are generally made of glass or silicon, due to their chemical inertness. Nonetheless, flexible printed circuit boards (PCB) based on polyimide and copper films have been recently used as substrates by some groups, due to the fact that they allow flexible device fabrication, and also due to their low cost[22,23]. The contact electrodes are either metallic (*e.g.* gold, copper, aluminium, chromium) or other conductive materials (*e.g.* Indium-Tin-Oxide, doped silicon). Furthermore, the dielectric layer may be composed of Parylene, SU-8 or polydimethylsiloxane (PDMS). The hydrophobic layer is typically made of Teflon® or Cytop®[1,24]. Finally, the filler is generally oil, which allows for lower actuation voltages and prevents droplet evaporation[2].

1.1.2. Electrowetting-on-dielectric

The most common approach to DMF relies on the electrowetting-on-dielectric (EWOD) effect. To explain this effect, let us consider a conductive liquid droplet (*e.g.* water) standing on a non-conductive solid material (*e.g.* dielectric). In this configuration, several interfaces are present, namely the solid-liquid interface, the liquid-gas interface and the solid-gas interface. The triple contact line is defined as the line along which all 3 phases are in contact. By applying voltage between the droplet and the bottom of the dielectric layer, charge redistribution will be induced along the interface between both materials (liquid droplet and dielectric surface), creating an electric double layer (EDL)[25]. These charges will then exert lateral pressure at the vicinity of the contact line, due to charge repulsion, and if the interface is deformable, as is the case in study, spreading of the liquid will occur, thus inducing a change in the contact angle[10,25]. This change in contact angle with the applied voltage (V) may be described by the Lippmann-Young equation[26]:

$$\cos\theta = \cos\theta_0 + \frac{C}{2d\gamma_{\mathrm{LG}}}V^2 \tag{1.1}$$

Where θ_0 is the initial contact angle, θ is the contact angle after voltage application, γ_{LG} is the liquid-gas surface tension, d is the dielectric thickness and C is the dielectric capacitance.

It is also noteworthy that, if alternating voltage is applied, the voltage V in equation 1.1 should be replaced by its root mean square value (V_{RMS}).

1.1.3. Digital Microfluidics for nucleic acid amplification

DMF has several interesting applications, namely in the fields of medicine and biotechnology, with microfluidic immunoassays, chemical microreactors, proteomics, diagnostics and also DNA manipulation (*e.g.* extraction, purification, hybridisation, amplification)[1]. DNA amplification is particularly relevant for the present work, which is why this type of DNA manipulation will be emphasized, while other DMF applications to DNA control may be consulted in the above-mentioned bibliography.

DMF has been widely used for a variety of nucleic acid-related applications, such as extraction and purification of RNA[27] and DNA[23], nucleic acid sequencing[28] or real-time hybridisation monitoring[29]. However, due to the nature of this work, DMF devices for nucleic acid amplification will be focused.

Nucleic acid amplification is one of the most relevant tools in molecular biology, allowing the monitoring of gene expression, quantification of food-borne pathogens, diagnostic of hereditary and infectious diseases, as well as numerous forensic analysis processes[30]. The first theoretical description of a nucleic acid amplification technique dates back from 1971, when Kleppe *et al.*[31] worked on *developing methods for the synthesis of high molecular weight bihelical DNA with specific nucleotide sequences*. However, it was not until 1985 that Mullis *et al.*[32] successfully achieved the first technique for nucleic acid amplification: the polymerase chain reaction. Since then, other amplification techniques have been developed, namely nucleic acid sequence-based amplification (NASBA), signal mediated amplification of RNA technology (SMART), strand displacement amplification (SDA), loop-mediated isothermal amplification (LAMP) and others[33].

Particularly, DMF devices have been proved to bring several advantages over standard DNA amplification, namely reagent volume reduction, minimisation of the analysis time and the possibility of process automation[1]. The first group to achieve DNA amplification with DMF platforms was the Chang group[34], by amplifying a detection gene for the Dengue II virus via PCR. With this DMF platform, Chang *et al.* were able to successfully amplify a sequence of the Dengue-II virus (511 base pairs) in 55 minutes, with a total sample volume of 15 µL. Finally, it should be noted that the droplet actuation voltage and frequency were relatively low: 12 V_{RMS} at 3 kHz.

Another example of DNA amplification using digital microfluidics was developed by Hua *et al.*[35] that established a DMF platform for real-time multiplexed PCR, fabricated by low-cost microfabrication processes. This group developed a fully integrated system, comprised of a control/detection section and a disposable sample processing section. With this DMF platform, the Hua group performed real-time PCR detection of methicillin-resistant *Staphylococcus aureus* (MRSA), *Mycoplasma pneumoniae* and *Candida albicans*. MRSA was used to test the system sensitivity, and it was verified that amplification was possible using just one copy of MRSA genomic DNA. This same DNA was used to optimise the speed of the PCR process, and it was found that variable cycle dwell times (10 s for cycles 1 to 25, 30 s for cycles 25 to 35 and 20 s for cycles 36 to 40) yielded a faster process – 18 minutes in total – with no significant changes in performance (threshold cycle and final reaction product) from the standard 30 s cycle time. Finally, since there are four distinct regions for amplification, multiple PCR processes

were performed simultaneously, and successful detection of MRSA and *M. pneumoniae* was possible.

Several other examples of DMF platforms for nucleic acid amplification may be found in the literature[36–42], however, the majority of the platforms rely on PCR, which requires thermal cycling at 3 different temperatures and therefore makes the platform design excessively complex. In annex 1, a comparison between these platforms is available.

In light of the aforementioned facts, it is easily uncovered the lack of a novel DMF device for simple nucleic acid amplification via loop-mediated isothermal amplification, which would have an enormous potential for point-of-care genetic diagnostics.

1.2. Loop-Mediated Isothermal Amplification

Loop-mediated isothermal amplification (LAMP) is an isothermal nucleic acid amplification technique developed by the Notomi group[43] in 2000, which allows up to a 10^9-fold amplification of a target DNA sequence in just 1 hour, at a relatively low temperature (60 °C to 65 °C). A typical LAMP assay involves 5 main elements: two inner primers, two outer primes and a DNA polymerase with considerably high strand displacement activity. In order to explain the working principle of the technique, let us consider one strand of a target double stranded DNA sequence which comprises the following regions: 1) B3, B2 and B1 near the 5' end and 2) F3c, F2c and F1c on the opposite end. The outer primer F3 is complementary to F3c, whereas the outer primer B3 is identical to the B3 region of the target DNA. The inner primers (FIP – forward inner primer, and BIP – backward inner primer) consist of two joint sequences each, one of which is complementary to the target DNA sequence (F2, B1c) and the other is identical to the target sequence (F1c, B2). Firstly, following a denaturation step, FIP, which is in higher concentration than F3, hybridises to F2c and primary DNA synthesis is carried out in the 5'-3'direction. F3 then hybridises to F3c in the target DNA and a secondary DNA synthesis process is initiated. Since the DNA polymerase has strand displacement ability, the primarily synthesised DNA strand (p-DNA) is separated from the target sequence, thus allowing the secondary synthesis to be completed. The p-DNA strand contains two complementary regions on the 5' end, which hybridise to one another, forming a loop. Secondly, a similar DNA synthesis process occurs on the p-DNA strand, with B3 and BIP primers, resulting in the formation of a dumb-bell structure. The fore-mentioned reaction stages represent the first step in LAMP, the starting material production step.

The cycling amplification step begins with the elongation of the 3' end of the dumb-bell structure, since this region is perceived as a primer by the DNA polymerase, a phenomenon known as self-priming. Furthermore, FIP and BIP continue to hybridise to their complement regions throughout amplification and elongation steps, producing a concatenated DNA string with several loops, containing repeats of the target sequence, and also other by-products[43–45]. Figure 1.2 illustrates the various steps in a LAMP reaction.

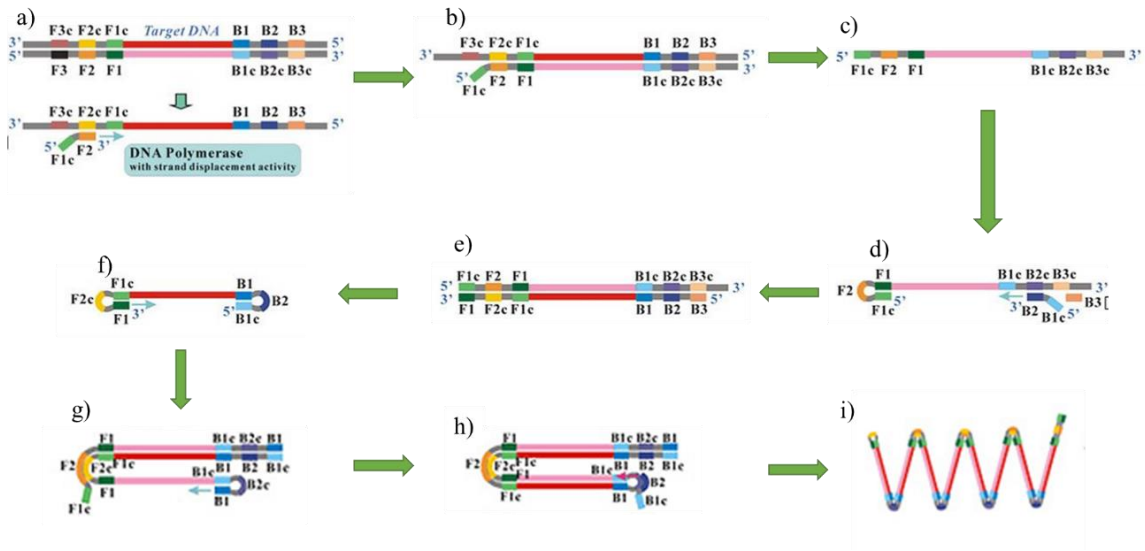

Figure 1.2: Schematic representation of a LAMP process: a) FIP bonding to the 3´DNA end; b) complementary strand synthesis by DNA polymerase; c) single-stranded DNA, complementary to the template DNA strand (p-DNA); d) formation of a loop structure at the 5' end and beginning of a new DNA strand synthesis on the opposite end; e) formation of a new DNA strand, equal to target DNA; f) looping of both DNA strand ends, due to base complementarity, generating a dumb-bell-like structure and g) to i) new DNA synthesis from the looped 3' and 5' structures, leading to DNA amplification. Adapted from reference 46.

This innovative method offers many advantages over the preferential DNA amplification technique, PCR, such as an exceptionally high amplification efficiency, overall simplicity and lower energy requirements (a single temperature is required), and also high sensitivity[43]. In annex 2, a comparative table between both techniques may be found.

Recently, several groups have developed conventional microfluidic platforms which aim to produce micro LAMP (µLAMP) reactions[47–49]. µLAMP offers several advantages over bench-top reactions, such as specific and faster reactions, requiring lower sample/reagent volumes. Moreover, due to the possibility of fully automatic reactions, with no human intervention, µLAMP has the potential of reducing the number of false-positive assays and its sensitivity has been reported to be similar to that obtained in bench-top reactions[44].

Having this in mind, the main purpose of this thesis is to join both DMF and µLAMP techniques in a novel and innovative device. This device will be the first to perform DNA amplification by the LAMP method via a DMF chip with an original design, and it will also include a novel and exceptionally straightforward method of inserting and extracting samples in/from the chip: entry ports will be drilled on the top plate, partially overlapping the sample reservoirs.

2. Materials and Methods

2.1. DNA extraction

The first step required for nucleic acid amplification is the production of the target DNA sequence (*c-Myc*, in this case). As such, *Escherichia coli* (*E-coli*) bacteria containing a plasmid harbouring a fragment of the human *c-Myc* gene were inoculated in 100 mL of Luria-Bertani (LB) medium, to which 200 µL of ampicillin (Sigma Aldrich) was added, and incubated under constant agitation, at 37 °C, for 14 hours. Following incubation, alkaline lysis was performed (see annex 3 for details), in order to extract DNA from the bacteria. A PCR reaction was later performed, as to determine if the extracted DNA indeed corresponded to *c-Myc*. PCR was performed for 20 µL, with 0.4 mM dNTPs each (Fermentas), 1 µM F3 and B3 (StabVida), 0.04 U/µL *Taq* Polymerase, 1x DreamTaq™ buffer (both from ThermoFisher Scientific) and 10 ng/µL of extracted DNA. For the PCR reaction, an initial denaturation was performed, at 95 °C for 5 min., followed by 20 amplification cycles, each comprising: 1) 30 s denaturation at 95 °C, 2) 30 s annealing at 62 °C and 3) 30 s elongation at 72 °C. A final elongation step was performed, at 72 °C for 5 min.

2.2. Previous study of the LAMP technique

To the best of my knowledge, DNA amplification by the LAMP technique has never been achieved on a digital microfluidics platform. As such, it is of utmost importance to thoroughly study this process before applying it to a DMF device, namely to assess its limits and capabilities. For all the tests mentioned below, the LAMP reaction was performed according to the procedure described by Notomi *et al.*[43] (for precise reagent description, see annex 4), in a total reaction volume of 20 µL, with the exception of the volume limit study. Briefly, each LAMP master mix contained 400 µM each dNTPs, 0.8 µM of FIP and BIP, 0.2 µM of F3 and B3, 1 M betaine, 4 mM $MgCl_2$, 1x enzyme buffer and 0.32 U/µL *Bst*. Prior to each assay, the master mix was prepared, containing all the reagents required for the LAMP reactions, except for the target DNA. For the positive control assays, 19 µL of the reaction mix were added to 1 µL of target DNA, whereas for the negative control, 19 µL of the reaction mix were added to 1 µL of pure water.

Firstly, in order to determine the optimal LAMP reaction time, 20 µL reactions were performed in a thermal cycler (DNA Engine Peltier Thermal Cycler - Bio-Rad) for 30 min., 45 min. and 60 min., at 65 °C, with both positive and negative controls per reaction time. All positive controls contained 0.5 ng/µL DNA concentration. Secondly, as to understand how sensitive the LAMP technique is, 20 µL reactions were performed in the same thermocycler for 60 min. and 90 min., at 65 °C, where positive controls include sequential 10-fold dilutions ranging from a 0.5 ng/µL initial DNA concentration until a 0.05 pg/µL initial DNA concentration. Furthermore, to study the effect of volume reduction, LAMP reactions were implemented in different reaction volumes, namely 20 µL, 15 µL, 10 µL, 5 µL, 2.5 µL, 2 µL and 1.25 µL, for 60 min. and 90 min. reaction time each, at 65 °C. For this study, all reaction volumes were withdrawn from an initial mix containing LAMP reagents at appropriate concentrations (see annex 4) and 0.5 ng/µL DNA concentration. For reaction volumes equal to, or inferior to 5 µL, 5 µL of mineral oil (Sigma-Aldrich) were added. A temperature study was also performed, as to identify the optimal reaction temperature, for 55 °C and 60 °C, during 60 minutes and 90 minutes, for 20 µL as reaction volume and DNA concentrations of 5 pg/µL and 0.5 pg/µL. Finally, the LAMP reaction kinetics was studied in real time by adding 1 µL of EvaGreen (Biotium) fluorophore to the LAMP master mix (the total volume was maintained with water volume reduction) and analysing the fluorescence of the samples with a real-time detection system (Rotor-Gene 6000 - Corbett) for the same DNA concentrations as for the limit of detection study, at 65 °C.

2.3. Device design and fabrication

For the bottom-plate, first of all, two different mask configurations were designed using CorelDRAW X7® software and printed on high-resolution emulsion film photomasks (the latter was performed by JD Photodata, UK). These masks contained the pattern for the chromium electrodes, connection lines

and pads, which were printed to glass substrates by photolithography. Before proceeding to the photolithographic process itself, the glass substrates were thoroughly cleaned by immersing the substrates in acetone, isopropyl alcohol and pure water containers, which were placed in an ultrasound bath, for 15 minutes each. As for the lithography process, the glass substrates were initially covered with AZ6632 1.2 µm grade photoresist (MicroChemicals), by spin-coating (Model WS-650MZ-23NPP – Laurell) at 2000 rpm for 10 s, followed by 4000 rpm for 20 s. The substrates were then placed on a hot plate (Isotemp – Fisher Scientific) at 115 °C, for 75 seconds. Following the prebake process, the substrates were roughly aligned in a mask aligner (Karl Suss), since only one step of photolithography was required, and exposed to UV light in the same apparel for an optimised time of 5 s. Finally, the photoresist was revealed using AZ726 MIF developer (MicroChemicals), for an optimised time of 35 s, and the substrates were then immersed in pure water to stop the developing process and dried by a nitrogen jet. After patterning, a 200 nm chromium layer was deposited on the substrates, at 100 °C, by means of a home-made electron-beam (e-beam) evaporation system. Following chromium deposition, lift-off was performed. The substrates were first placed in an acetone bath and were carefully agitated, to facilitate chromium removal. This step was repeated for another two acetone baths, until full dissolution of the photoresist, and samples were then cleaned with isopropyl alcohol and pure water. The lift-off process was controlled visually with the aid of a magnifier (Leica M80), and whenever necessary, a fine brush was used to help remove photoresist (and chromium). A 2 µm* layer of the dielectric, Parylene C (CAS 28804-46-8), was then deposited on the substrates, by means of a chemical vapour deposition system (SCS Labcoater® - PDS 2010). Finally, a 50 nm* hydrophobic layer of Teflon® AF 1600 (DuPont) was deposited over the dielectric layer. For this purpose, a solution containing 0.6% wt/wt of Teflon® AF 1600 in Fluorinert FC-40 (DuPont) was spin-coated at 1000 rpm for 30 s, with a coating acceleration of 100 rpm/s, followed by baking at 160 °C for 10 minutes. The top plate consisted of a glass substrate coated with a 100 nm layer of Indium-Tin-Oxide (ITO), in which holes were mechanically drilled with a diamond tip, partially overlapping the reservoir areas. This plate was further coated with Teflon®, following the procedure described above. The gap between plates was maintained at approximately 180 µm, by using 3 layers of Kapton® tape (PPC216 - Farnell). This thickness was confirmed by using a digital micrometer (IP65 - Mitutoyo). Finally, silicone oil (Baysilone® M350 – Siff Chemicals) was used as a filler medium between plates.

2.4. Device characterisation

In order to study the dielectric behaviour of Parylene C, several capacitors were fabricated, by depositing a layer of Parylene C between two crossed layers of chromium, which in turn were deposited by physical evaporation with a home-made e-beam, thus forming a metal-insulator-metal (MIM) structure. The dielectric behaviour (dielectric constant and loss tangent) was analysed over frequency, by means of an impedance analyser (4294A Precision Impedance Analyser – Agilent). Furthermore, an electrode control system, as well as a temperature control system (thin film ITO thermoresistor plus control hardware and software) were adapted to the DMF platform and the latter was further tested, to evaluate its performance and determine the temperature gradient along the chip thickness and the vertical axis of a reaction droplet. In order to do so, real time temperature measurements were performed for 3 bottom plate temperature levels (50 °C, 60 °C and 65 °C). Temperature was measured on both bottom and top plates, by using a thermocouple directly connected to the temperature control system and another thermocouple connected to an AD595 amplifier and a multimeter (Fluke 45 dual display), respectively. Both thermocouple signals were recorded on a computer using a Matlab® script. Finally, a brief evaluation of the DMF platform was performed, where the novel input/output method was analysed, as well as all the fluidic operations and the average droplet velocity. Droplet velocity was determined for both device configurations, by averaging droplet head and tail velocities during the droplet transition from one electrode to the following.

2.5. LAMP on device

LAMP on-chip was performed by adding 8 droplets of LAMP mix reagents to 1 droplet of DNA solution, at either 4.4 ng/µL or 56.5 ng/µL, guaranteeing an initial DNA concentration of 0.5 ng/µL or

* All the signalled thicknesses were measured using an Ambios XP-Plus 200 Stylus profilometer.

an initial DNA amount of 10 ng, respectively (trials 1 and 2). Each droplet presented a volume of 0.18 µL (see section 3.3.1), yielding a final reaction volume of 1.62 µL. Trial 1 was initially tested for a 60 min. reaction time and bottom plate temperature of 63 °C. Trial 1 was further tested for 65 °C as bottom plate temperature, with a total 60 min. reaction time. Trial 2 was also tested with the latter conditions. Furthermore, the on-chip LAMP reaction time was studied, where LAMP reactions were performed for 15 min., 30 min. and 45 min., with a bottom plate temperature of 65 °C and initial DNA concentration of 0.5 ng/µL.

3. Results and Discussion

3.1. DNA extraction

In order to understand whether the DNA extraction had been successful, that is, if the extracted DNA indeed corresponded to *c-Myc*, a PCR reaction was performed, by resorting to the LAMP outer primers (F3 and B3). Each reaction tube had a final volume of 20 µL and contained 0.4 mM dNTPs (each), 1 µM F3/B3, 0.04 U/µL *Taq* Polymerase and 1x DreamTaq^{TM} buffer. The positive control also contained 0.5 ng/µL of extracted DNA. 20 cycles were completed, with 95 °C for denaturation, 66 °C for annealing and 72 °C for polymerisation. Figure 3.1 depicts the electrophoretic analysis performed to the final PCR products, resorting to 1% (m/v) agarose gel.

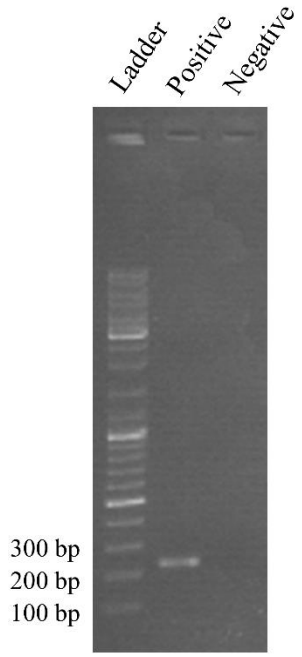

Figure 3.1: Electrophoretic analysis of the PCR-amplified extraction product, including positive and negative controls, in comparison with a DNA ladder.

Resorting to the outer primers, an amplicon size of 229 base-pairs (bp) was expected (see annex 4) from a PCR reaction. As can be seen on figure 3.1, the band on the positive control is located between the 200 bp and 300 bp bands, and it is slightly closer to the 200 bp band, which indicates that the amplicon size is a match to the *c-Myc* fragment delimited by the outer primers.

Having the correct target DNA, the following step of my work was the study and comprehension of the LAMP reaction.

3.2. Study of the LAMP reaction for DMF

In this section, the LAMP reaction will be thoroughly studied, as to determine the best reaction parameters for further adaptation of the technique to the DMF chip. In particular, LAMP reaction time, limit of detection, volume and temperature will be evaluated, and finally, a real-time analysis of the reaction will be performed.

3.2.1. Reaction time analysis

It is of utter importance understanding exactly how much reaction time is required to obtain a reliable, detectable result. As such, 3 reaction times were initially studied (30 min., 45 min. and 60 min.), with a constant initial DNA concentration of 0.5 ng/µL, a constant temperature of 65 °C and a volume of 20 µL. Figure 3.2 depicts the results of the electrophoretic analysis.

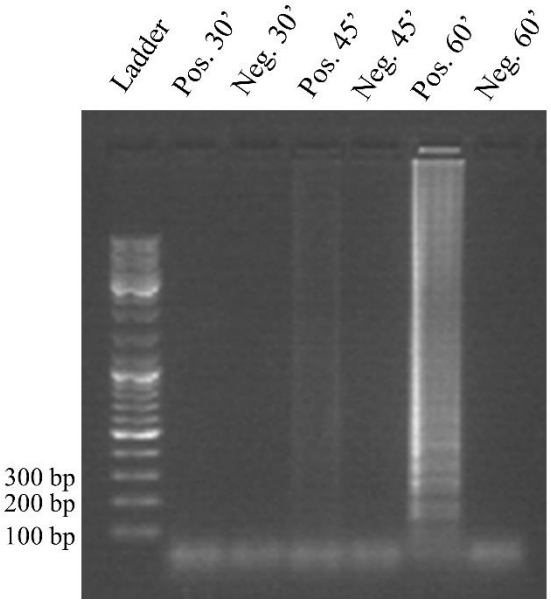

Figure 3.2: Electrophoretic analysis of the LAMP products obtained for the reaction time analysis (30 min., 45 min. and 60 min.), in comparison with a DNA ladder.

Briefly, there was successful amplification for 45 min. and 60 min. reaction time, but not for 30 min. reaction time. Comparing the positive controls for 45 min. and 60 min., it is clear that the band for 60 min. reaction time is brighter than the band for 45 min. reaction time, suggesting that DNA amplification was more efficient for 60 minutes, producing a higher amount of DNA. On this first LAMP reaction analysis, it is also noteworthy that LAMP products diffuse along the full extent of the lanes, which indicates the presence of several amplification products with various sizes, called concatemers (see section 1.2). A summary of the LAMP reaction time study may be consulted on table 3.1.

Table 3.1: Summary of the results obtained for the study of the LAMP reaction time. "Y" indicates that there was DNA amplification and "N" indicates that there was no amplification.

Temperature	Time	Volume	Initial DNA concentration	Result
65 °C	30 min.	20 µL	0.5 ng/µL	N
	45 min.			Y
	60 min.			Y

3.2.2. Determination of the reaction limit of detection

Determining the limit of detection (LOD) in a LAMP reaction allows us to identify the minimum target DNA concentration required for the LAMP reaction to occur. If the amount of initial DNA is too small, the probability of LAMP primers colliding with target DNA and triggering the reaction is also small. However, if the initial DNA concentration is too high, the LAMP reaction can be inhibited. In order to determine the LOD for this particular reaction, LAMP was performed for 20 µL, with successive 10-fold dilutions of target DNA, ranging from 0.5 ng/µL to 0.05 pg/µL, constant temperature (65 °C) and variable reaction times (60 min. and 90 min.).

From the electrophoretic analysis (figure 3.3), it is possible to conclude that, for 60 min. reaction time, DNA amplification is possible for all initial DNA concentrations, except for 0.05 pg/µL. Even so, amplification for an initial DNA concentration of 0.5 pg/µL had a low efficiency, judging from the very faint vertical band in figure 3.3. Nevertheless, for 90 min. reaction time, even 0.05 pg/µL of initial DNA concentration yielded successful amplification. This was an expected result, since even if we have a small initial DNA concentration, which results in a lower probability of gathering the

required conditions for amplification to occur (primer hybridising to the target sequence, DNA polymerase binding to this sequence and beginning of polymerisation), with longer reaction times, at some point, these conditions will be respected. LAMP reactions with further decrease in initial DNA concentration were not performed, since it would result in unnecessary DNA detection. That is, even if the reaction allows detection of lower DNA concentrations, it would be irrelevant to detect a single *c-Myc* strand, for example, since such a low DNA quantity would not be indicative of cancer (the *c-Myc* gene exists in healthy humans, it is its overexpression that is related to cancer). It is also visible that, for 60 min. reaction time, the vertical bands tend to become dimmer as initial DNA concentration decreases, indicating a lower final DNA concentration. This is also expectable, since higher initial DNA concentration leads to an earlier start of the LAMP reaction. As such, the effective LAMP reaction is actually longer for higher DNA concentrations. However, this does not happen for 90 min. reaction time, as the vertical band for 5 pg/µL is considerably brighter than all others. A possible explanation for this phenomenon is that a LAMP reaction, as any other reaction, has optimal conditions, which result in an output maximisation and therefore, 5 pg/µL as initial DNA concentration may lead to an optimal LAMP output in the test conditions (65 °C and 90 min.).

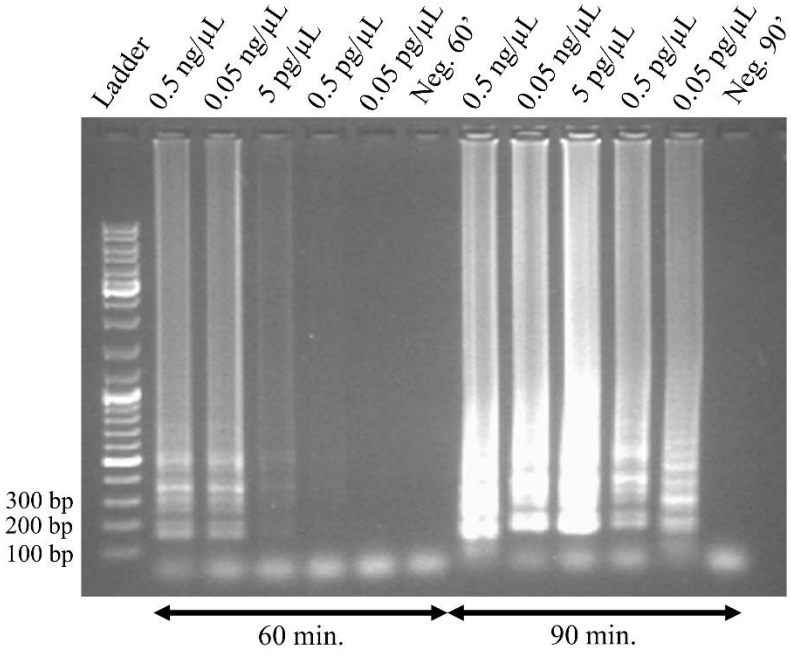

Figure 3.3: Electrophoretic analysis of the LAMP products for reaction detection capabilities, with 60 min. and 90 min. reaction times, in comparison with a DNA ladder. 10-fold dilutions were performed for initial DNA concentrations ranging from 0.5 ng/µL to 0.05 pg/µL.

Table 3.2 summarises the results obtained for this particular study.

Table 3.2: Summary of the results obtained for the study of the limit of detection in the LAMP reaction. "Y" indicates that there was DNA amplification and "N" indicates that there was no amplification.

Temperature	Time	Volume	Initial DNA concentration				
			0.5 ng/µL	0.05 ng/µL	5pg/µL	0.5 pg/µL	0.05 pg/µL
65 °C	60 min.	20 µL	Y	Y	Y	Y	N
	90 min.		Y	Y	Y	Y	Y

3.2.3. Analysis of the reaction volume

One of the major concerns about performing a LAMP reaction on a DMF platform is the effect that a significant volume reduction would have on the amplification process. To the best of my knowledge, most µLAMP devices resort to 20 µL - 30 µL reaction volumes[44], whereas only a few[47,49] work with a

reaction volume inferior to 5 µL. The DMF platform proposed in this work is designed to work with low reaction volumes (see section 3.3.1), therefore an initial reaction volume study was performed, as to understand if DNA amplification would still be possible with significant volume reduction. Moreover, 5 µL of mineral oil was added to reaction volumes of 5 µL or inferior, in order to prevent evaporation, which becomes a crucial issue for smaller volumes. Preventing evaporation will also be essential for any reaction performed on the DMF platform proposed, therefore silicone oil will be used as a filler medium. As such, for a preliminary study, it will also be relevant to analyse the effectiveness of adding oil to the bench-top LAMP reaction in terms of liquid evaporation.

All reactions were performed at 65 ℃, for 60 min. and 90 min., with an initial DNA concentration of 0.5 ng/µL and volumes ranging from 20 µL down to 1.25 µL. Figure 3.4 shows the electrophoretic analysis of all the LAMP products obtained.

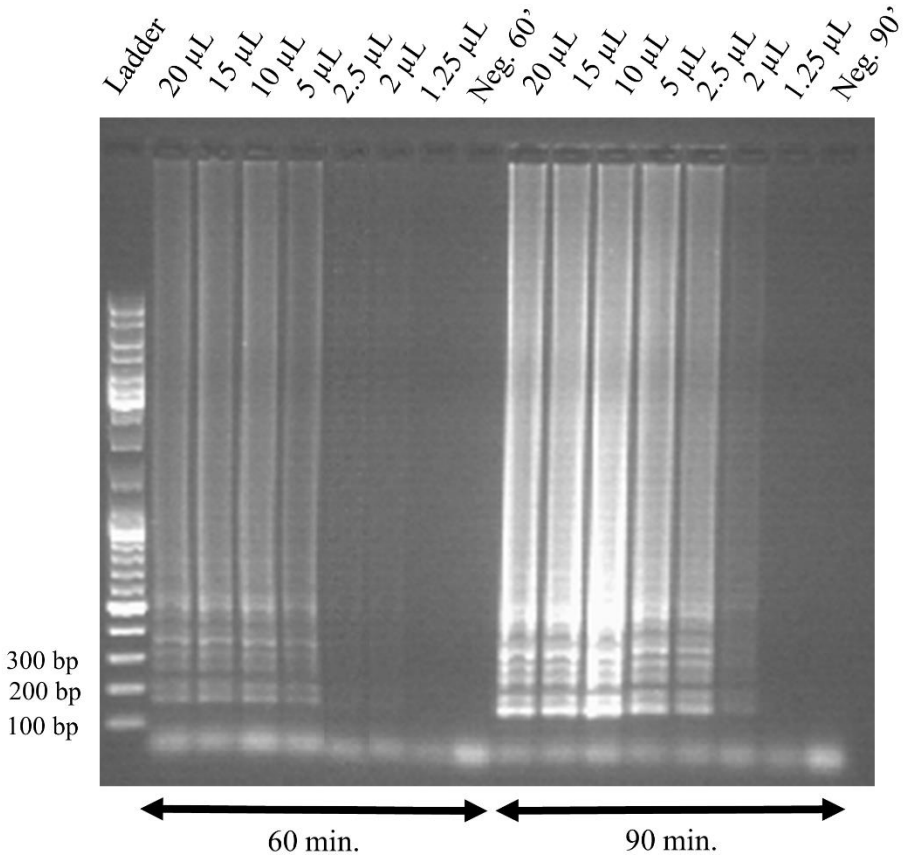

Figure 3.4: Electrophoretic analysis of LAMP products obtained for the study of reaction volume reduction, with 60 min. or 90 min. reactions, in comparison with a DNA ladder.

For both reaction times, DNA amplification was possible until a minimum volume of 2 µL. For 60 min. reaction time, there is a significant reduction in band brightness from 5 µL to 2.5 µL reaction volume, which indicates a decrease in amplification efficiency. Since all reagents were withdrawn from the same master mix, it is likely that the decrease in amplification efficiency is a direct consequence of volume reduction. Reducing the volume even further (1.25 µL) resulted in no amplification at all. There are several possible justifications for this issue: 1) there could be a possible mix between the liquid fraction and the oil, considering that the reaction volume is extremely low, which interfered with the enzyme activity and 2) using such a low reaction volume could have resulted in a decrease of the reagents' diffusion effect, which would hinder the LAMP reaction.

For 90 min. reaction time, there is a reduction in band brightness from 2.5 µL to 2 µL. Again, longer reaction time leads to a higher amplification efficiency, which is why higher final concentrations are attained, even with volume reduction. Furthermore, it is important to state that there were no visible

signs of evaporation (air bubbles or reduction of the intended volume), which indicates that using oil to cover the aqueous solution is an effective way to reduce volume loss.

Table 3.3 presents a summary of the results obtained for the study of the LAMP reaction volume.

Table 3.3: Summary of the results obtained for the analysis of the reaction volume in the LAMP reaction. "Y" indicates that there was DNA amplification and "N" indicates that there was no amplification.

Temperature	Time	Volume	Initial DNA concentration	Result
65 °C	60 min.	20 µL	0.5 ng/µL	Y
		15 µL		Y
		10 µL		Y
		5 µL		Y
		2.5 µL		Y
		2 µL		Y
		1.25 µL		N
	90 min.	20 µL	0.5 ng/µL	Y
		15 µL		Y
		10 µL		Y
		5 µL		Y
		2.5 µL		Y
		2 µL		Y
		1.25 µL		N

3.2.4. Reaction temperature analysis

Temperature is a key factor in a LAMP reaction, and typically, DNA amplification using this method occurs within the range of 60 °C to 65 °C. This narrow temperature range is directly related to the enzyme used in LAMP, *Bst* polymerase, which presents low thermostability. As such, the temperature used for LAMP must fall into the *Bst* working temperature range, and even small temperature deviations may result in sub-optimal regimens of reaction, and ultimately no amplification[43].

Temperature is also relevant from the DMF platform point of view. Preliminary studies performed on other DMF devices at CENIMAT indicate that deionized water droplets start to evaporate at temperatures just above 65 °C, even with the use of oil as a medium filler, producing micro-air bubbles which in turn are prejudicial to droplet movement. Moreover, higher temperatures require more power, and subsequently, more energy consumption. Therefore, an effort to reduce the LAMP reaction temperature as much as possible would be relevant, not only to prevent evaporation, but also to reduce the DMF platform energy requirements.

Since the previous LAMP reactions occurred at the optimal LAMP reaction temperature, 65 °C, the temperature analysis was performed for 60 °C and 55 °C, with two different initial DNA concentrations: 5 pg/µL and 0.5 pg/µL, for a volume of 20 µL and a reaction time of 90 min. The electrophoretic analysis of the LAMP products is shown on figure 3.5. Briefly, amplification occurred for both DNA concentrations at 60 °C, however, no amplification was possible at 55 °C. Since amplification is possible for 60 °C, it would be interesting to test this lower amplification temperature on-chip. However, considering that the purpose of this work is to present a proof-of-concept, the ideal temperature for LAMP on-chip reactions will be set as 65 °C, the optimal LAMP temperature.

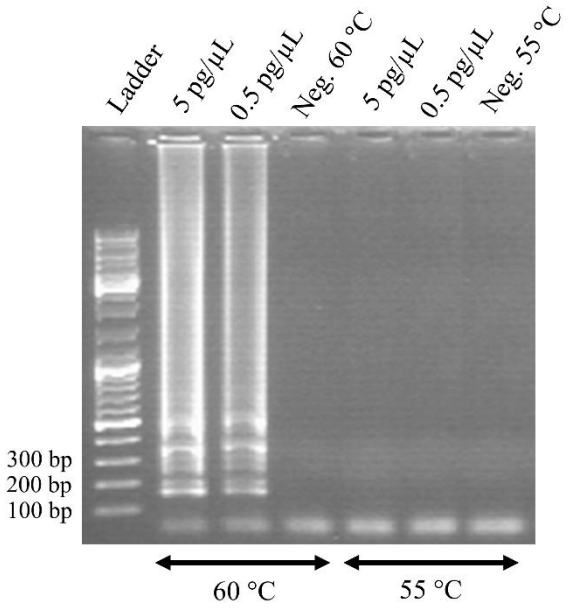

Figure 3.5: Electrophoretic analysis for the LAMP temperature study, in comparison with a DNA ladder. LAMP reactions were performed with the following conditions: 60 °C, with 5 pg/µL and 0.5 pg/µL initial DNA concentrations and 55 °C, with 5 pg/µL and 0.5 pg/µL initial DNA concentrations.

A summary containing all the results from the LAMP reaction temperature analysis may be found below, on table 3.4.

Table 3.4: Summary of the results obtained for the analysis of the LAMP reaction temperature. "Y" indicates that there was DNA amplification and "N" indicates that there was no amplification.

Temperature	Time	Volume	Initial DNA concentration	
			5 pg/µL	0.5 pg/µL
60 °C	90 min.	20 µL	Y	Y
55 °C			N	N

3.2.5. Summary of LAMP parameters for on-chip reactions

In brief, it is possible to conclude that all the variables tested (temperature, volume, time and initial DNA concentration) influence the outcome of a LAMP reaction. Below 60 °C, there is no amplification, and initial DNA concentrations under 0.5 pg/µL only result in amplification for 90 min. reaction time. Moreover, reaction times under 45 min. yield no amplification, and it is possible that significant volume reduction yields reaction inhibition, since there is no amplification visible for a reaction volume of 1.25 µL, regardless of the tested reaction times. All the other conditions result in DNA amplification. An on-chip LAMP reaction obviously occurs in a different environment than that of a bench-top reaction, however, it was necessary to pre-establish a starting point for on-chip reactions, which would facilitate the on-chip reaction optimisation. As such, considering the previous LAMP study, primary on-chip LAMP conditions will be set as: 1) 0.5 ng/µL of initial DNA concentration; 2) a reaction volume close to 2 µL; 3) 65 °C as reaction temperature, with the possibility of experimenting slightly lower temperatures and 4) 60 min. reaction time.

3.2.6. Real-time LAMP analysis

Understanding the behaviour of a certain reaction with time is also important to understand the limits and capabilities of the considered reaction (LAMP in this case). Moreover, the real-time LAMP analysis is also of great relevance for future developments of this work: integrating impedance measurements on the DMF device and follow the LAMP reaction on-chip, in real time, by means of the impedance variation resulting from DNA amplification. As such, real-time LAMP was performed

for initial DNA concentrations ranging from 0.5 ng/µL to 0.05 pg/µL with 10-fold dilutions, at 65 °C (figure 3.6). Each cycle presented in figures 3.6 a) and b) corresponds to 1 min., which means that the number of cycles is equal to the reaction time, in minutes.

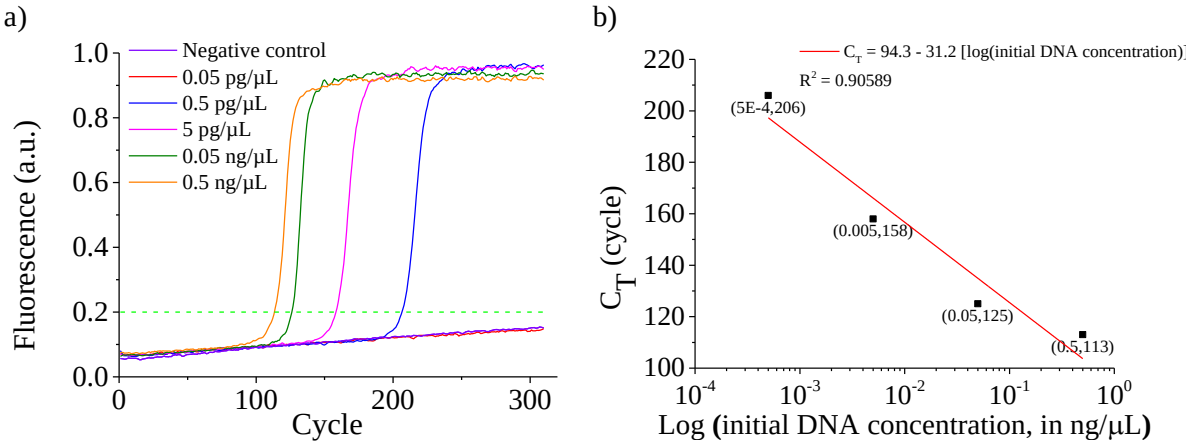

Figure 3.6: a) Real-time LAMP analysis for several initial DNA concentrations, at 65 °C. The horizontal green dashed line indicates the fluorescence level chosen to determine the threshold cycles. b) Threshold cycle variation with initial DNA concentration. Each cycle corresponds to 1 min.

Firstly, this analysis clearly shows that LAMP is an exponential reaction, and shortly after the beginning of DNA amplification, there is an extremely steep enhancement of fluorescence, as can be seen on figure 3.6 a), indicating a very high amplification speed (about 20/25 min. between the beginning of the reaction and maximum amplification). It is also visible that every reaction attains a fluorescence plateau at approximately the same level, which suggests that regardless of initial DNA concentration, the final DNA concentration is roughly equal. The amplification process is therefore inhibited as of a maximum DNA concentration. To the best of my knowledge, there have been no exhaustive studies of real-time LAMP, which narrows the ground for reasoning on the limited range of amplification observed. Clearly, further studies would be required to test all the possible hypotheses. For example, for higher initial DNA concentrations, the LAMP reaction starts earlier, which is expectable, since the probability of a primer hybridising to a single DNA strand is higher. However, considering that each initial DNA concentration is 10 times more diluted than the previous one, it would be expectable that the fluorescence curves were equally spaced in time. In this case, the fluorescence curves become more spaced as initial DNA concentration decreases. A possible justification for this issue is poor dilution accuracy, that is, due to the error associated with pipettes, more/less volume of either water or DNA solutions might have been pipetted, which, at this scale, would produce significant differences in DNA concentration. Another incoherent finding is the fact that LAMP reactions with initial DNA concentrations of 0.5 ng/µL to 0.5 pg/µL were previously studied for 60 min. and 90 min., at 65 °C and the electrophoretic analysis indicated higher final concentrations than the ones obtained for the same reaction times in real-time analysis. There are three possible explanations for this phenomenon: 1) LAMP notably relies on the strand displacement activity of the *Bst* polymerase. For real-time study of a reaction, a fluorophore is usually added to the reaction mix, in this case, EvaGreen. EvaGreen is an intercalating dye, which binds between two DNA strands (double helix) and emits fluorescence. However, this intercalating agent could interfere with the strand displacement activity of the DNA polymerase, thus retarding the LAMP reaction. 2) The device used for real-time LAMP (Rotor-Gene 6000 - Corbett) has a lower efficiency in temperature control, which means that small temperature variations can occur and influence the reactions. 3) This study was performed about 3 months later than the previous ones, and during this time spam, DNA degradation could have occurred.

It is noteworthy that even after 5 hours, the negative control, as well as the 0.05 pg/µL DNA sample, produced no visible amplification.

Moreover, the threshold time for the LAMP reactions was determined for 20% of the amplification process (figure 3.6 b). Summarily, 20% of the LAMP reaction is completed in 113 min., 125 min.,

158 min. and 206 min. for 0.5 ng/µL, 0.05 ng/µL, 5 pg/µL and 0.5 pg/µL initial DNA concentrations, respectively.

3.3. Platform design and operation

After having studied the LAMP technique, and determining the starting conditions for on-chip LAMP assays, the DMF chips were designed and fabricated. In this section, the specific layouts of the chips are presented, as well as the additional hardware, software and generic procedures required to perform LAMP reactions.

3.3.1. Device layout

As was mentioned before (see section 2.3), the DMF chip consists of a two-plate configuration on glass substrate, where the bottom plate includes chromium electrodes covered by a Parylene C dielectric layer, which in turn is covered by a Teflon® hydrophobic layer. The top plate consists of a glass substrate, covered by ITO and Teflon®, where inlet/outlet ports were drilled, to allow sample or reagent insertion/withdrawal from the chip. The space between bottom and top plates is maintained by three overlapped pieces of Kapton® tape, with approximately 60 µm thickness each, yielding a final spacing of approximately 180 µm.

The first step in device fabrication involves defining exactly what will be the final device layout. I propose a T-shaped design, with four major regions (figure 3.7): 1) a reservoir for LAMP reagents; 2) another reservoir for the DNA samples; 3) a mixing region, where LAMP reagents will be mixed with the DNA sample, and where LAMP reactions will occur and 4) a retrieving reservoir, from which reaction products will be withdrawn from the device.

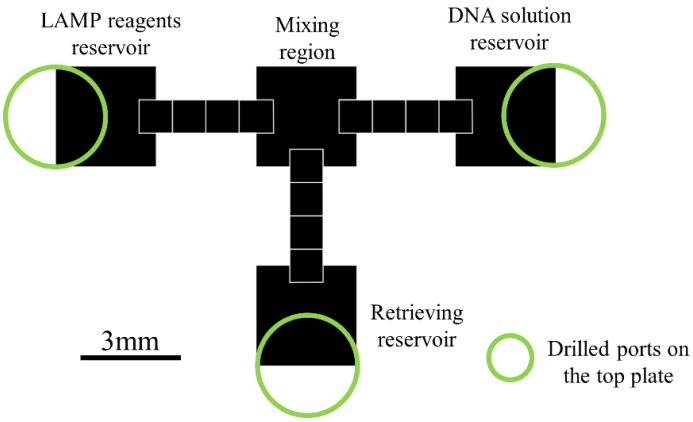

Figure 3.7: Digital microfluidics device layout, evidencing the various regions that comprise the chip, as well as the location of the inlet/outlet ports, drilled on the top plate.

First of all, it is important to adapt the mixing region to the final reaction volume. Let us consider, for instance, that two small droplets originating from the reservoirs are moved towards a large mixing region. Arriving at the mixing region, it will be rather difficult to move them towards the centre of the mixing area, therefore mixing will also be difficult. Even if the mixing is successful, it would be arduous to remove the droplets from the mixing region, since the electric field of nearby electrodes would have to be strong enough to pull the droplets from the centre of a relatively large mixing region. Secondly, the electrode shape is rather important to facilitate droplet movement and reduce operating voltages. Having this in mind, I propose the following designs:

- Configuration A, which relies on standard square reservoirs and electrodes. The mixing region is about the same size as the reservoirs, as to accommodate LAMP reactions. Figure 3.8 a) and c) show the layout of this configuration.
- Configuration B is a novel, innovative design that relies on zig-zag shaped electrodes. It is well known[10,21] that using crenelated electrodes significantly improves droplet motion, since one of the major obstacles for droplet movement, gap hydrophobicity, is overcome. In brief, DMF requires

multiple electrodes, which must be separated so that each of them may be addressed individually. The gap between electrodes creates a hydrophobic region over which droplets must pass in order to attain the neighbouring electrode. The idea behind using crenelated electrodes is to place some indentations belonging to one electrode inside the area of another electrode, as to force the droplet to occupy the full area of the electrode it is standing on and, at the same time, occupy some of the area belonging to the next electrode. Nevertheless, the fabrication of such small features is not cost effective, and presents a low yield, therefore, as an alternative, I propose the use of larger, zig-zag shaped electrodes, which would ideally allow the same concept of overlapping (figure 3.8 b,d). This configuration includes two different electrode layouts: 1) half zig-zag shape*[1], corresponding to the electrodes closest to the reservoirs and mixing region and 2) full zig-zag shape*[2], corresponding to the remaining electrodes. The half zig-zag shape allows the improvement of droplet dispensing, since there is a larger electrode area near the reservoirs.

Additional configurations were designed (see annex 5), however, these configurations were not thoroughly tested.

Figure 3.8 and table 3.5 indicate the device's layout and design specifications.

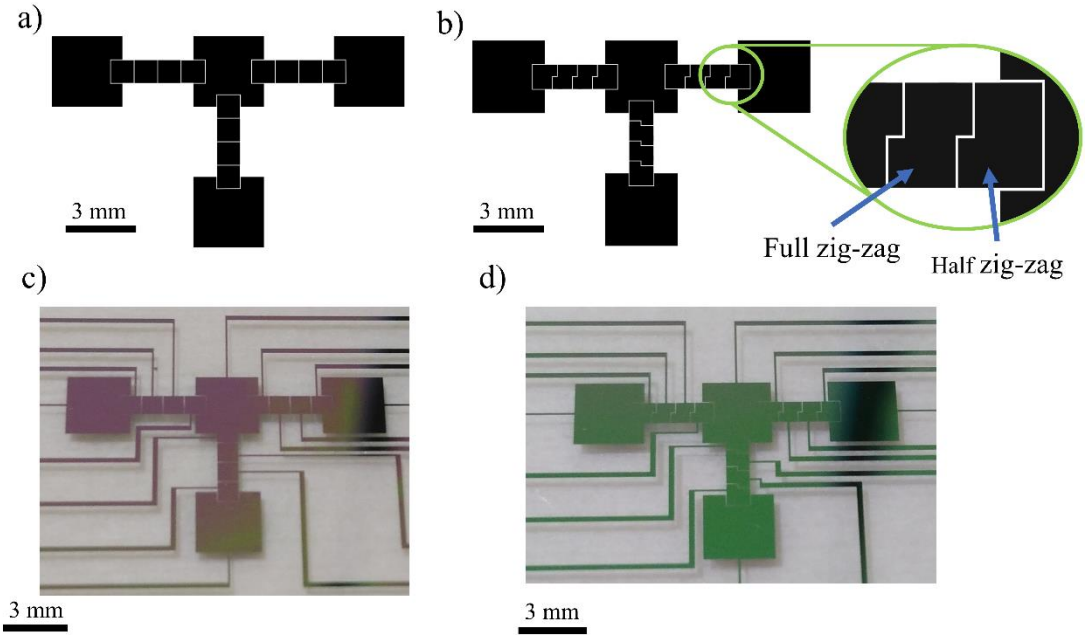

Figure 3.8: Proposed device configurations: a) configuration A; b) configuration B, with emphasis on the full zig-zag and half zig-zag electrodes; c) photograph of a configuration A device; d) photograph of a configuration B device.

Table 3.5: Device specifications for each configuration.

	Configuration A	Configuration B
Electrode area (mm^2)	1	0.894*[1]/0.794*[2]
Electrode shape	Square	Full/half zig-zag
Mixing region area (mm^2)	9	9
Mixing region volume (µL)	1.62	1.62
Reservoir area (mm^2)	9	9
Reservoir volume (µL)	1.62	1.62
Droplet volume (µL)	0.18	0.16*[1]/0.14*[2]
Gap between electrodes	30 µm	
Space between bottom and top plates	180 µm	

3.3.2. Digital Microfluidics platform operation: required external hardware and droplet manoeuvring on-chip

The DMF chip itself relies on a number of structures to assure its operation. First of all, the DMF device requires a physical support. This support, based on the work of Fobel *et al.*[50], was printed previously in a 3D printer, and it includes designated spaces for an ITO thin film heating resistor (responsible for generating heat), an HD camera, which enables real-time visualisation of all fluidic operations and contact pogo pins, which allow addressing of each electrode individually. In order to address an electrode/reservoir, an AC signal is necessary. This signal is generated by a signal generator (TG1000 10MHz DDS function generator - TTi), and it is further amplified 200 times by a high voltage amplifier (Model PZD700A - TREK). The signal from the high voltage amplifier is then processed by a High Voltage Switching Unit[50], which enables an ON state (high voltage) or OFF state (ground) for each electrode/reservoir on the chip, according to the commands given by an Arduino (Arduino MEGA) control board. This control board is in turn controlled by home-made Matlab® software on a computer, which allows the user to order the state (ON or OFF) of each electrode/reservoir (16 independently addressable electrodes). In annex 10, a full description of both Arduino and Matlab® software used for electrode/reservoir driving may be found. The connection between the High Voltage Switching Unit and the DMF chip is granted by connection pogo pins attached to the platform's physical support. Figure 3.9 shows an overview of the DMF system as a whole.

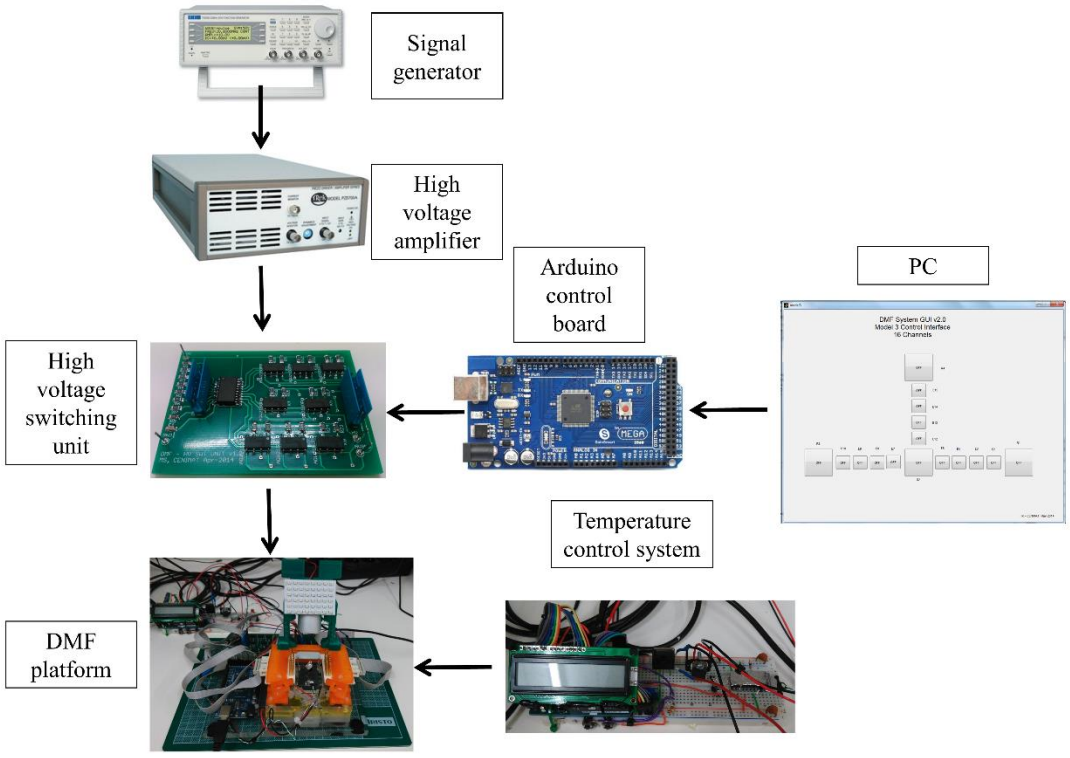

Figure 3.9: Overview of the DMF platform, as well as the associated hardware.

Furthermore, an independent temperature control system designed in-house was added, to deliver the temperature necessary for LAMP reactions. Temperature is provided by the ITO thin film heating element, however, a control system is required, in order to achieve and maintain the temperature setpoint. This system consists of a thermocouple (as a temperature sensor) connected to an AD595 amplifier, and its output is in turn connected to an Arduino board (Arduino UNO). A PID (proportional-integral-derivative) software controller loop further commands a pulse width modulation (PWM) signal to a power transistor, which delivers the output power to the heating element. This controller prevents temperature deviations thanks to a feedback mechanism which continuously compares the actual temperature with the setpoint value. If the actual temperature is higher/lower than the setpoint, the control system automatically decreases/increases the power applied to the heating

element, to maintain the setpoint. The entire temperature control system is powered by 9 V via a power supply (PL303 Power Supply – TTi). A precise description of the temperature control system is available on annex 6, and the characterisation of the ITO thin film resistor may be consulted on annex 7.

The above-mentioned hardware allows the performing of on-chip LAMP reactions, however several steps must be followed in order to successfully manipulate the samples and completing the reaction (figure 3.10), namely: 1) inserting both DNA sample and LAMP reagents on the appropriate reservoirs, through the drilled ports, by means of a pipette; 2) applying an electric potential (activating) the reservoirs, to allow the spreading of the droplet within the reservoir; 3) activating the electrodes nearest to the reservoir and deactivating the reservoir itself, as to allow the dispensing of part of the droplet; 4) spreading the droplet along the 3 nearest electrodes to the reservoirs, creating an "arm"; 5) deactivating the middle electrode, between the reservoir and the last activated electrode, and activating the reservoir, to produce a pinching effect, which will result in cutting the "arm", thus creating a smaller droplet; 6) moving the small droplets towards the mixing region, by activating the electrodes near the mixing region, and the mixing region itself; 7) mixing both solutions, by pushing the resulting droplet back and forth along the vertical axis of the device. This is achieved by successively activating electrodes on the path towards the withdrawal reservoir, deactivating the mixing region and then deactivating the electrodes, as well as activating the mixing region. In this case, for each LAMP reaction, 8 droplets of LAMP mix were added to 1 droplet of DNA solution, in a sequential manner, that is, LAMP mix was first moved towards the mixing region, and then the DNA solution droplet was added.

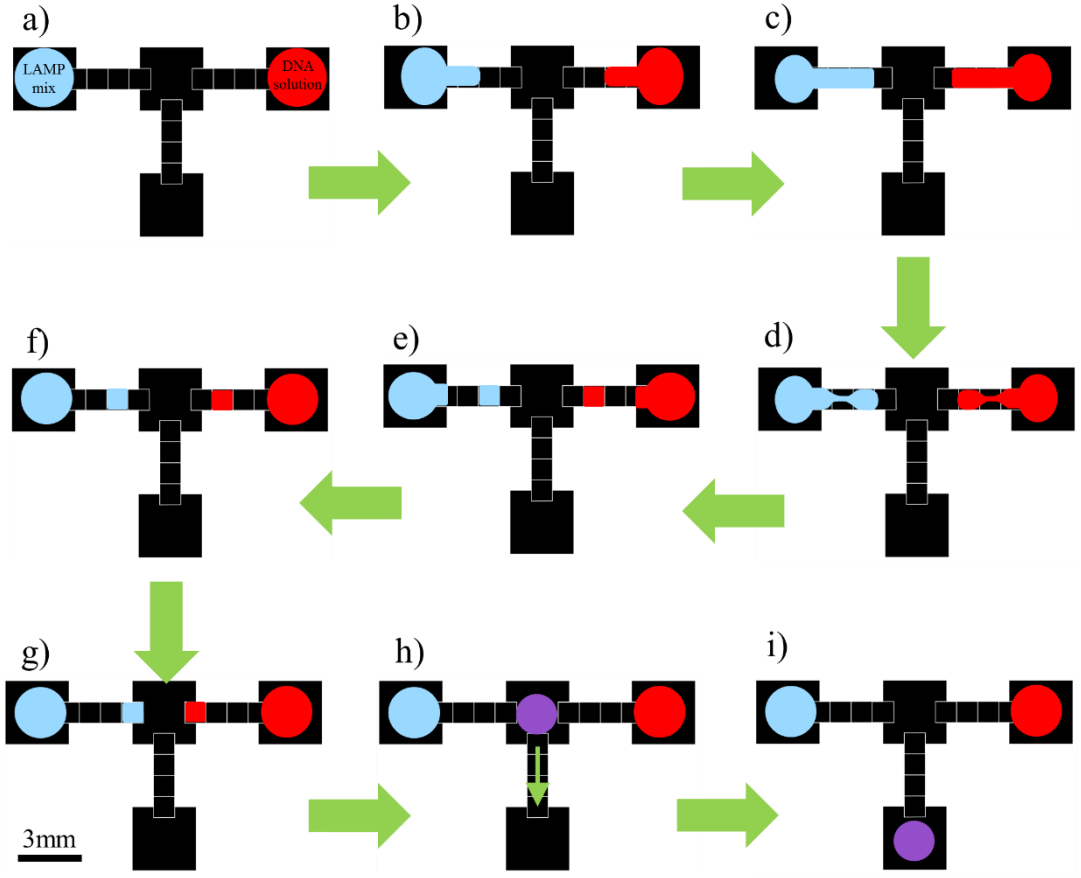

Figure 3.10: Generic steps required to perform a LAMP reaction on the proposed DMF device: a) insertion of both LAMP reagents and DNA solution on opposed reservoirs; b) dispensing of a droplet "arm" from the reservoirs; c) stretching of the droplet "arm"; d) liquid pinching, due to deactivation of the cutting electrode; e), f) pulling of the droplet "arm", which leads to the formation of single droplets (splitting of a droplet from the remaining liquid); g) moving single droplets towards the mixing region; h) merging of the two single droplets and mixing them with back and forth movements and i) moving the resultant droplet towards the retrieving reservoir.

3.4. Platform characterisation

Platform characterisation is essential before proceeding to LAMP reactions on-chip, in order to understand the behaviour of all the elements that comprise the device and evaluate the platform capabilities for effectively performing a LAMP reaction.

3.4.1. Parylene C characterisation as a dielectric

The dielectric layer is one of the most important layers in a DMF device, especially for chemical/biotechnological purposes, since it prevents water electrolysis[26]. Also, by adding a dielectric layer with a reasonable dielectric constant, we are enlarging the number of charges that can be accumulated in the vicinity of the dielectric. As was explained earlier, the electrowetting effect relies on the accumulation of charges on the base of the droplet, which in turn forces the liquid-gas interface to deform and the droplet spreads. Therefore, a reasonable dielectric constant implies an easier droplet spreading. Parylene C is a suitable candidate for a PoC platform based on DMF, since it is biocompatible[51], has low permeability to moisture, possesses good dielectric properties[52] and its deposition process allows conformal, pinhole-free coatings[53]. Following previous work[54] done at CENIMAT, an ideal thickness of 2 µm is proposed for the dielectric thickness. This particular thickness allows a relatively low theoretical operating voltage (40 V) and a reasonable difference between operating and dielectric breakdown voltages (48 V). Dielectric breakdown occurs when the applied electric field is strong enough to free electrons which were bound to atoms from the dielectric. These newly-freed electrons are then accelerated by the electric filed and may collide with other bound electrons with enough strength to pull them from the range of the corresponding atoms. This process is disseminated as a chain reaction, leading to an avalanche breakdown. As a result, conductive paths are formed in the dielectric material, thus annulling its insulating nature. In practice, dielectric breakdown enables water electrolysis, which consumes solution droplets, and would possibly damage the electrical control system, due to power overload. As such, the thickness of Parylene C was chosen to allow a good margin in operation voltage, and at the same time maintain a relatively low minimum theoretical operation voltage.

For characterisation purposes, several capacitors were produced on a glass substrate, with Parylene C as a dielectric and chromium electrodes in a cross configuration (MIM-like structure, as described by the schematic on figure 3.11), in order to mimic the conditions of the DMF platform. The capacitors were individualised prior to electrical characterisation. For further details on the fabrication of the capacitors, see annex 8.

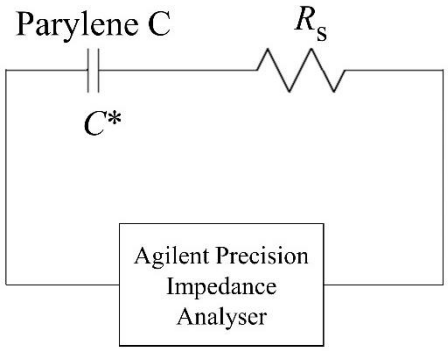

Figure 3.11: Schematic model for the Parylene C dielectric and the series contact resistance, as measured by the impedance analyser.

Figure 3.12 shows the behaviour of Parylene C relative permittivity and loss tangent with frequency. The behaviour of the capacitor may be divided into two regimes: a lower frequency regime (100 Hz to 100 kHz), where the dielectric nature of the capacitor is dominant (Parylene C), and a higher frequency regime (above 100 kHz), where the impedance of the series contact resistance (chromium electrodes plus probe contact) is dominant over the capacitive high frequency impedance.

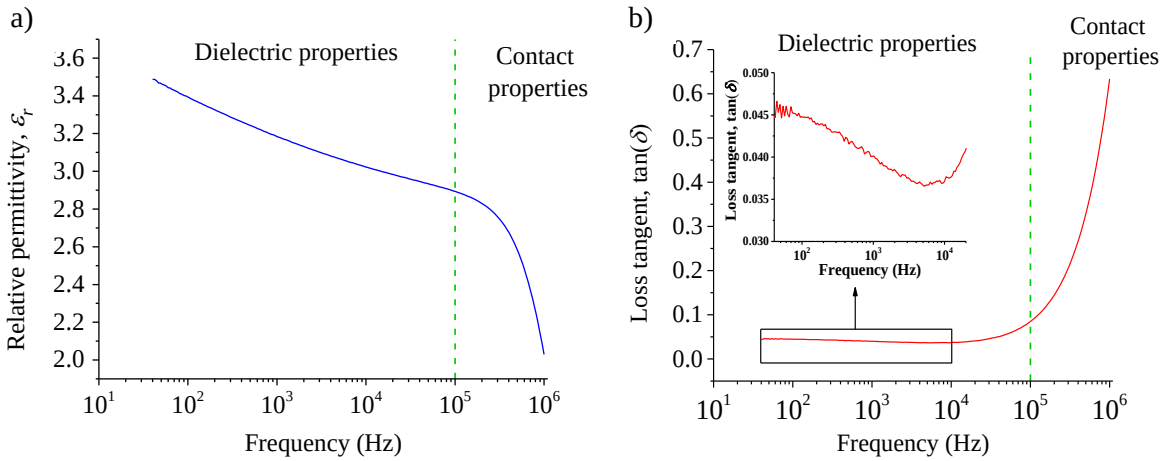

Figure 3.12: Behaviour of the Parylene C capacitor with frequency, in terms of relative permittivity (a) and loss tangent (b). The green dashed line indicates the approximate division between the regime where dielectric properties are dominant, and the regime where contact resistance properties are dominant.

Regarding the low frequency regime, figures 3.12 a) and b) show an evident decrease in the dielectric constant and a spreading peak in the loss tangent. This behaviour is typical of a low frequency dielectric relaxation in Parylene C, which spreads over a large range of frequencies, as can be confirmed by the literature[52]. As the frequency increases, the Parylene C capacitive impedance becomes smaller, until the resistive behaviour of the contact electrodes becomes dominant.

By fitting the data with the mathematical model of the circuit depicted on figure 3.11 at high frequencies (see annex 8), it is possible to determine the value of the series resistance associated to the electrode contact resistance: between 22.5 Ω and 23.5 Ω.

At 5 kHz in particular (working frequency of the DMF device), the Parylene C relative permittivity was determined to be 3.07, which is very close to the value determined in the literature[52] for the same conditions, 3.00 (4% error). At this frequency, the loss tangent presents a value of 0.037.

3.4.2. Temperature control evaluation on the Digital Microfluidics platform

As was mentioned earlier, temperature control is of keen importance in a LAMP reaction. In bench-top LAMP reactions, temperature control typically relies on a Peltier element placed under honeycomb microtube entrances, which allow uniform temperature distribution throughout the samples. In the DMF platform proposed, heat is produced by a thin film resistor placed under the bottom plate, which means that heat must be transferred through the bottom plate substrate until reaching the reaction droplet, which could be a potential problem. As such, some tests were performed to determine the temperature gradient across a reaction droplet, in order to guarantee that all on-chip LAMP reactions occur within the optimal temperature range (60 °C to 65 °C). Figure 3.13 shows the experimental setup for the temperature tests. In brief, temperature measurements were performed both at the bottom (T_1) and top plates (T_5), by means of two thermocouples. The bottom plate thermocouple is directly connected to the temperature control system, whereas the top plate thermocouple is connected to an AD595 amplifier, which in turn was connected to Matlab® software via a Fluke 45 dual display multimeter and a GPIB-USB cable for data recording. The hydrophobic, dielectric and electrode layers were omitted from all calculations and representations, since they are too thin in comparison to the glass substrates, or even the oil, and may be neglected. As such, for the following analysis, let us consider that heat produced by the thin film resistor will only be transferred through the bottom plate, oil and the top plate.

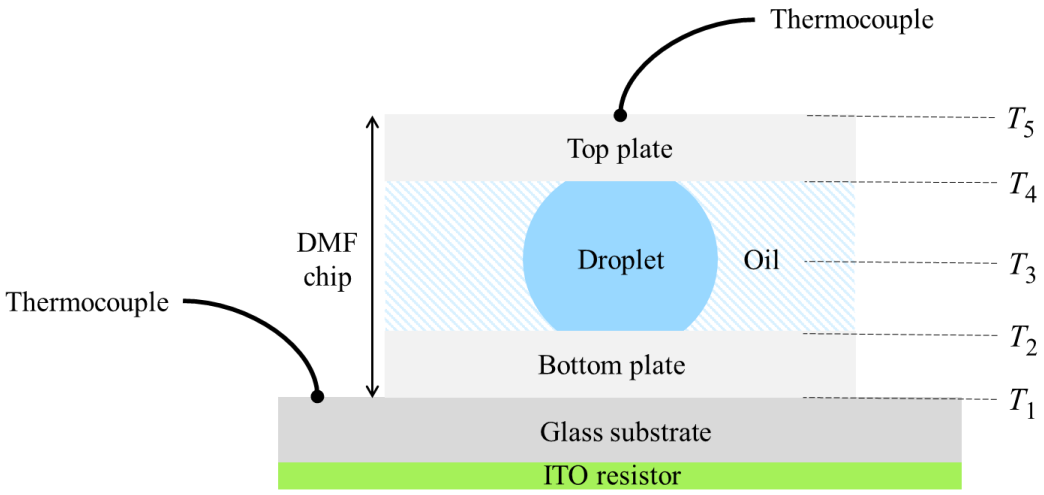

Figure 3.13: Schematic representation of the DMF platform, evidencing all the interfaces between different materials, to which correspond different temperatures, as well as the central device temperature (T_1 to T_5). This schema is not to scale.

3.4.2.1. Dynamic characterisation

The real-time behaviour of the temperature control system was evaluated for a temperature range from ambient temperature to 65 °C, with 3 constant bottom plate (T_1) temperature levels: 50 °C, 60 °C and 65 °C (figure 3.14). T_3 was determined simply as the average between inner bottom and top plate temperatures (T_2 and T_4), considering that the system is approximately symmetric, which is deemed a good approximation.

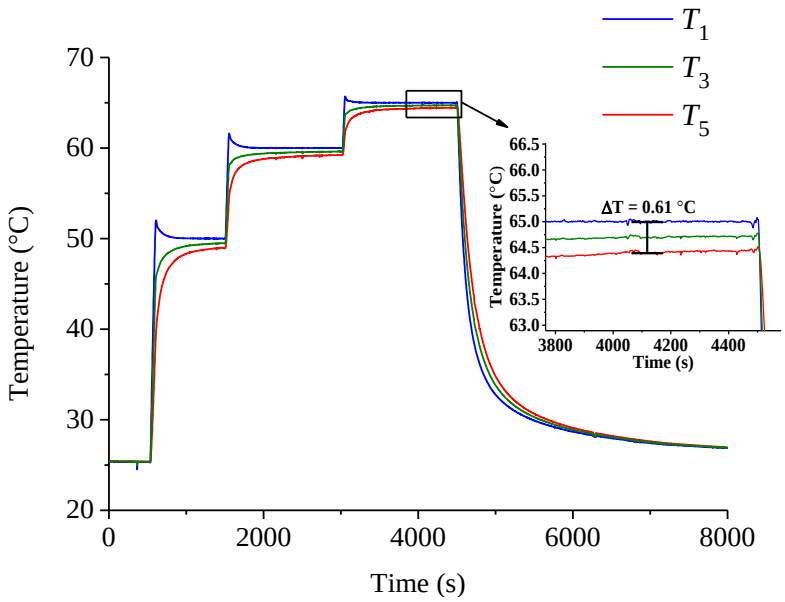

Figure 3.14: Evolution of temperature on the chip with time, namely T_1 (bottom plate), T_3 (centre of the chip) and T_5 (top plate).

The temperature rise in the thin film resistor is quite fast (only 200 seconds or 3.3 minutes were needed for the initial temperature rise, from ambient temperature to 50 °C, for instance) and heat is quickly transferred to the top plate. As temperature in the bottom plate approaches the setpoint temperature, there is a small overshoot, consequence of high speed controller settings, which is not visible in the top plate due to the thermal resistance of the materials between the points where T_1 and T_5 were measured. The PID controller was also proven to prevent temperature deviations, as was

intended, since the bottom plate temperature virtually presents no deviations from the setpoint after the overshoot phase.

3.4.2.2. Static characterisation

Regarding temperature evaluation on the DMF platform, the most important parameter to be studied is the temperature gradient across a LAMP reaction droplet. Since it is not possible to physically couple a temperature sensor to a single droplet, the temperature gradient was determined theoretically, as described below.

Since on-chip LAMP reactions should occur within the optimal temperature range, the droplet thermal gradient will be studied for bottom plate temperatures corresponding to both lower and higher temperature limits (60 °C and 65 °C). Let us consider first a bottom plate temperature (T_1) of 60 °C, to which corresponds a top plate temperature (T_5) of 59.1 °C (according to figure 3.14). Knowing the temperature values at T_1 and T_5, it is possible to determine the heat flow between both locations from an adaptation of Fourier's law, equation 3.1:

$$\frac{q}{A} = \frac{T_1 - T_5}{\frac{\Delta x_{glass}}{k_{glass}} + \frac{\Delta x_{oil}}{k_{oil}} + \frac{\Delta x_{glass}}{k_{glass}}} \tag{3.1}$$

Where q is the heat flow, Δx represents the thickness of each layer, A is the overlapping area of all layers involved and k represents the thermal conductivity for each material. Table 3.6 shows the various parameters of the material layers involved.

Table 3.6: Material parameters required for determination of the heat flow across a DMF device.

	Glass	Oil
Thickness[‡]	(0.959 ± 0.001) mm	(0.177 ± 0.001) mm
Thermal conductivity[55]	1.05 W/(m·K)	0.10 W/(m·K)

Solving equation 3.1 for a bottom plate temperature of 60 °C, we obtain a total heat transfer per unit area (q/A) of 250.2 W/m^2. Knowing the value of the heat flow, it is possible to determine any temperature from this system (T_1 to T_5). By determining T_2 and T_4, it is possible to know the gradient of temperature on a droplet during a LAMP reaction (table 3.7, setpoint 1).

Table 3.7: Temperature gradient across a DMF device, for average (200 measurements) bottom plate temperatures of 60 °C and 65 °C.

	Temperature (°C)		Measurement uncertainty[§]
	Setpoint 1	Setpoint 2	
T_1	60.0	65.0	
T_2	59.8	64.9	
T_3	59.6	64.7	± 0.1 °C
T_4	59.3	64.6	
T_5	59.1	64.4	

[‡] The uncertainties associated to the thickness were determined based on the maximum deviation from the mean value of 5 measurements (see annex 9).

[§] Uncertainty due to the dispersion of the values (standard deviation) plus the resolution of the measuring instrument.

For a bottom-plate temperature of 65 °C (table 3.7, setpoint 2), a total heat transfer per unit area of 166.9 W/m^2 was determined.

In conclusion, if the bottom plate temperature is set to 60 °C during a LAMP reaction, the droplets will undergo a vertical temperature gradient of about 0.5 °C, between 59.8 °C and 59.3 °C. If, however, the bottom plate temperature is set to 65 °C, then droplets will undergo a temperature gradient of 0.3 °C, between 64.9 °C and 64.6 °C. These results imply that the bottom plate temperature must be higher than 60 °C, otherwise the amplification reaction will occur below optimal thermal conditions (60 °C to 65 °C). Moreover, a measuring error of ± 0.5 °C is associated to the thermocouples, which must be taken into consideration. Nevertheless, it is possible to guarantee that the LAMP reactions occur in the optimal LAMP temperature range with one of the tested conditions. As such, the on-device LAMP conditions foreseen in earlier studies (section 3.2.5) are reaffirmed: on-device LAMP reactions ought to occur for a bottom plate temperature of 65 °C, which assures that the amplification reaction will remain in the optimal temperature range, even considering the thermocouple measuring error. Additionally, in one last attempt to lower the energy required for a reaction, I propose testing on-chip LAMP for a bottom plate temperature of 63 °C.

As was mentioned earlier, on section 3.3.2, further characterisation of the ITO thin film heating resistor may be found in annex 7.

3.4.3. Evaluation of platform performance

Before proceeding to the LAMP reactions on-chip, preliminary tests were performed to evaluate the performance of the DMF device, namely the novel droplet input system, operation voltages and frequencies, as well as fluidic operations.

3.4.3.1. Novel droplet input/output method

The novel input method was the first to be tested. As was mentioned before (see Motivation and Objectives), droplets are inserted directly onto the chip, by means of a pipette, which tip can pass through the drilled holes on the top plate. The output method relies on the same principle, making droplet insertion/removal extremely straightforward. Figure 3.15 shows a series of frames from a video, which show the droplet input process. This test was performed using 1x *Bst* enzyme buffer dyed with food dye, for better visibility. Droplets are first inserted through the ports, and then the respective reservoir is activated, allowing the droplet to spread over the reservoir. To withdraw droplets, the recovery electrode is turned off, making the droplet adhere to the walls of the port, and then a pipette may be used to pull the droplet.

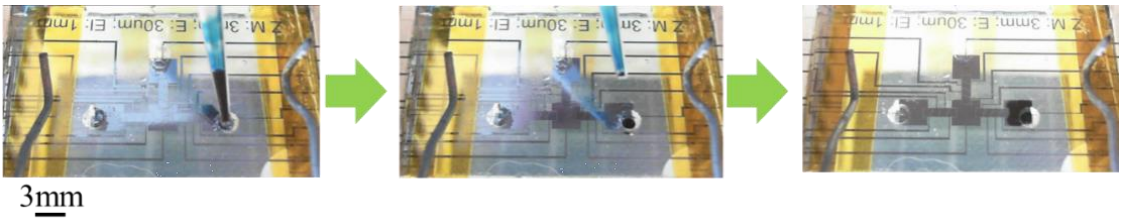

Figure 3.15: Sequential video frames, evidencing the sample input process.

3.4.3.2. Fluidic operations

Furthermore, all possible fluidic operations (dispensing, splitting, merging and mixing) were tested and successfully accomplished in this novel platform, as can be seen on figure 3.16. In this case, droplets also consist of dyed 1x enzyme buffer, to assure a better visibility.

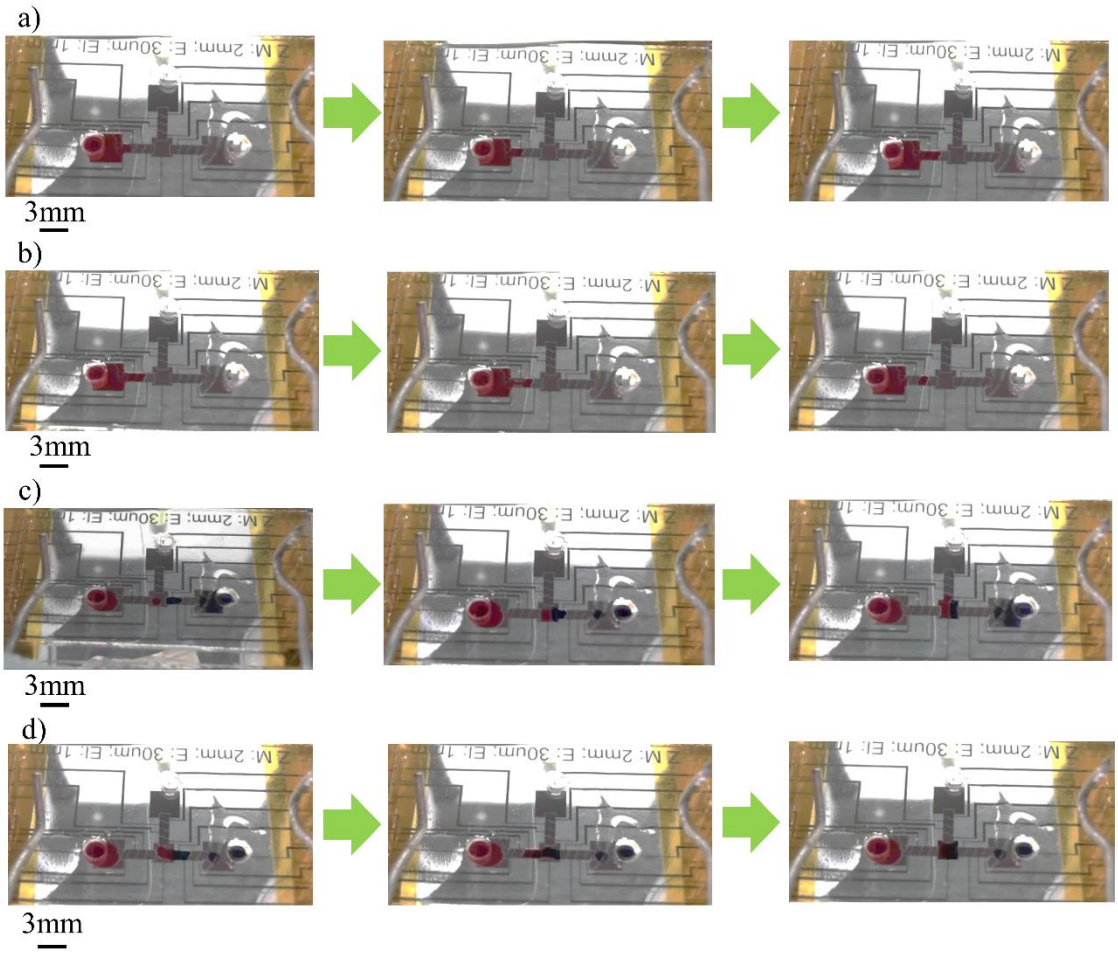

Figure 3.16: Video frames showing all the possible fluidic operations: dispensing (a), splitting (b), merging (c) and mixing (d).

Regarding operating conditions, namely working voltage and frequency, the two configurations were tested. Both configurations allow movement of 1x enzyme buffer droplets with 5 kHz and 50 V_{RMS} (standard operating parameters) at reasonable speed, with the possibility of lowering voltages until 12 V_{RMS} (see section 3.4.3.3). However, the zig-zag shaped electrodes do not work exactly as predicted. The original idea was for the droplet to fill the area of multiple electrodes. Nevertheless, due to surface tension, the droplet adapts itself to the shape of the electrode. Smaller features would be required to guarantee that the droplet overlaps multiple electrodes, as described in the literature[10].

The movement of a DNA solution (10 ng/µL) was also tested on-chip. However, it was not possible to move droplets at the working voltages (50 V_{RMS}), or even at higher voltages (up to 60 V_{RMS}). DNA had been suspended in ultra-pure water, with a very low ion content, therefore presenting an extremely high resistance (6.8 MΩ·cm). In order to move droplets by EWOD, it is required that liquid solutions have some conductivity, so that charges may accumulate on the base of the droplets and induce wetting, as was mentioned on section 1.1.2. If the droplets do not possess any free charges, or possess only a few charges (DNA is negatively charged), then it is not possible to generate enough pressure on the droplet-oil interface to induce wetting. To solve this problem, DNA was resuspended on 1x enzyme buffer. This does not have a negative effect on the LAMP reaction, since buffer concentration on the total reaction volume (LAMP reagents plus DNA solution) will remain unchanged. Droplets containing DNA resuspended on enzyme buffer are as easily movable as droplets containing LAMP reagents, which fully solves the droplet motion problem.

3.4.3.3. Droplet velocity

Droplet velocity is also an important parameter in DMF platforms. Higher droplet velocities are preferred, however, higher velocities usually require higher operating voltages, which could damage

the device. As such, a compromise between velocity and voltage must be achieved to guarantee the proper functionality of the DMF chip during the course of a reaction. In order to determine droplet velocity on a DMF platform, some phenomena must be taken into consideration: when a droplet moves from a non-activated electrode to an activated electrode, the interface closest to the activated electrode (droplet head) experiences a more intense electric field than the opposite interface (droplet tail). As such, the head is pulled first, and then the rest of the droplet follows the motion. This means that there are actually two different velocities that must be taken into consideration: 1) the head velocity and 2) the tail velocity. The real droplet velocity is determined by the average of both head and tail velocities. Figure 3.17 shows the average droplet velocities at several actuation voltages and a constant frequency of 5 kHz, for square and zig-zag electrodes. Velocity measurements were performed by determining how much time the droplet head/tail took to move from one non-activated electrode to an adjacent activated electrode, considering a total motion distance of: 1) 0.83 mm for zig-zag electrodes and 2) 1.03 mm for squared electrodes. The maximum uncertainties of the measurements were determined to be 10% of the measured value. Also, only 1x *Bst* enzyme buffer was used to perform velocity measurements, since LAMP reagents are quite expensive, and DNA samples are difficult to produce.

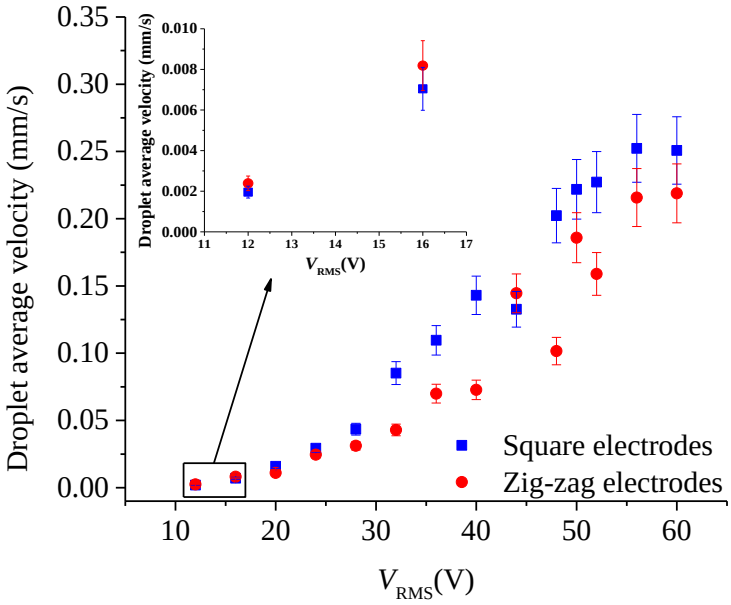

Figure 3.17: Droplet average velocity at several operating voltages and constant frequency (5 kHz), for both square and zig-zag electrodes.

In brief, square electrodes tend to yield higher droplet velocities than zig-zag electrodes, except for lower operating voltages, where there seems to be an inversion of this tendency. For square electrodes, a maximum velocity of (0.25 ± 0.03) mm/s was determined, for 60 V_{RMS}, and a minimum velocity of 0.0020 mm/s [(2.0 ± 0.2) µm/s] was determined for 12 V_{RMS}. For zig-zag electrodes, maximum/minimum velocities corresponding to the highest and lowest voltage limits were determined to be (0.22 ± 0.02) mm/s and 0.0024 mm/s [(2.4 ± 0.2) µm/s], respectively. Therefore, the novel electrode design seems to be slightly more advantageous than standard square electrodes, only for very low operating voltages. However, the determined droplet velocities are considerably lower than the ones described in the literature[56], which is likely due to the high viscosity of the silicone oil used in this work (350 cSt) in comparison to the oil viscosity typically used for DMF platforms[34,35,39] (1 cSt to 5 cSt). Furthermore, droplet motion is possible at very low actuation voltages (12 V_{RMS}), which is also an excellent achievement for such a recent DMF platform.

3.4.4. LAMP on-chip

After thoroughly studying both *c-Myc* LAMP amplification and chip functionality, the amplification reaction was transferred to the DMF device. All reactions were tested on configuration A devices, to

maintain a constant reaction volume. LAMP reactions had never been tested on DMF platforms, at such a smaller scale and different environment than a bench-top reaction. Therefore, two trials were initially posited in order to understand which one produced better results:

- Trial 1: maintain the initial DNA amount;
- Trial 2: maintain the initial DNA concentration.

Trial 1 was tested by adding 1 droplet of a DNA solution with 55.6 ng/µL and 8 droplets of LAMP mix, thus guaranteeing a total amount of 10 ng of DNA on a 1.62 µL reaction. The reaction occurred for 60 min., with 63 °C at the bottom plate, which would yield a reaction temperature closer to 60 °C. During the LAMP reaction, the mixing region was kept activated, to avoid unwanted droplet spreading, but with lower voltages, to prevent chip damage: 20 V_{RMS} at 5 kHz. The electrophoretic analysis of the LAMP products is represented on figure 3.18 a).

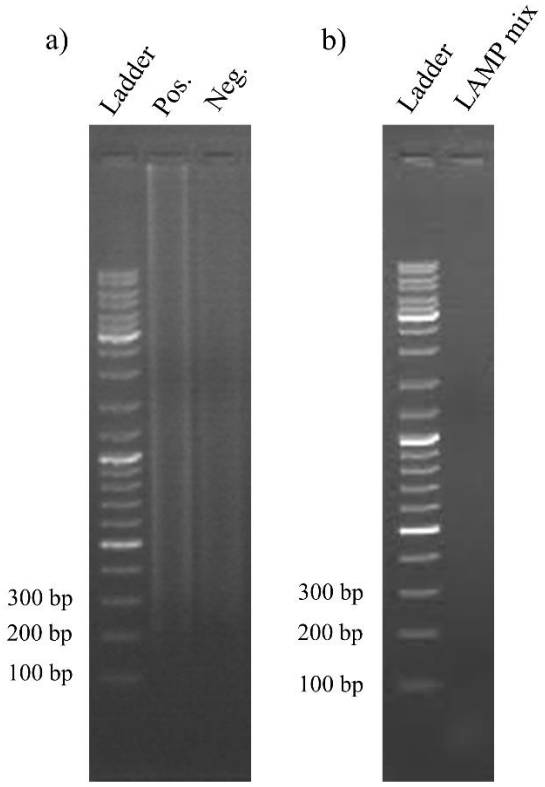

Figure 3.18: Electrophoretic analysis for LAMP on-chip products and reagents, in comparison with a DNA ladder: a) electrophoretic analysis for LAMP on-chip products, performed for 1.62 µL reaction volume, with 63 °C as bottom plate temperature and an initial DNA amount of 10 ng, for 60 min. b) Electrophoretic analysis for the LAMP master mix.

As can be verified on figure 3.18 a), for the first time it was possible to achieve DNA amplification by LAMP on a DMF platform, and therefore, the main objective of this thesis was accomplished. Nevertheless, DNA amplification is also detected for the negative control, indicating some kind of contamination. The negative control band in figure 3.18 a) is dimmer that the positive control band, which implies that the contaminating DNA is present in smaller concentrations than the *c-Myc* target sequence, for the current reaction conditions. In order to verify the origin of the contamination, 20 µL of the LAMP mix used for this test was also heated at 60 °C, for 60 min., in a bench-top thermocycler (DNA Engine Peltier Thermal Cycler - Bio-Rad). The electrophoretic analysis of the LAMP products is presented on figure 3.18 b), and it is possible to conclude that the initial LAMP mix was not contaminated, which suggests that the contamination originated on the DMF device. Another important finding is that both positive and negative control bands are relatively dim, which is why it was decided to use a higher temperature at the bottom plate, in order to improve the amplification efficiency. As from this assay, temperature at the bottom plate was kept at 65 °C, thus assuring that the LAMP reaction would always occur within LAMP ideal temperature limits (60 °C to 65 °C).

In order to solve the contamination problem, a biological cleaning procedure was implemented: prior to each on-chip LAMP reaction, both top and bottom plates were briefly immersed (about 30 s) in hydrogen peroxide, bleach and ethanol baths. Longer immersion times are not advisable, since hydrogen peroxide and bleach cause detachment of the Parylene C layer on the bottom plate, and degrade the ITO layer on the top plate.

Following this novel approach, trial 1 was tested once more, as well as trial 2. For trial 2, 1 droplet of DNA solution with 4.4 ng/µL was added to 8 droplets of DNA mix, thus guaranteeing a 0.5 ng/µL DNA concentration on the LAMP reaction. The total reaction volume was maintained at 1.62 µL. Similarly to the first on-chip reaction, 20 µL of the LAMP mix used for the reactions were withdrawn and underwent heating at 65 °C for 60 min. on the same bench-top thermocycler. Figure 3.19 a) shows the electrophoretic analysis of the LAMP products for both trials.

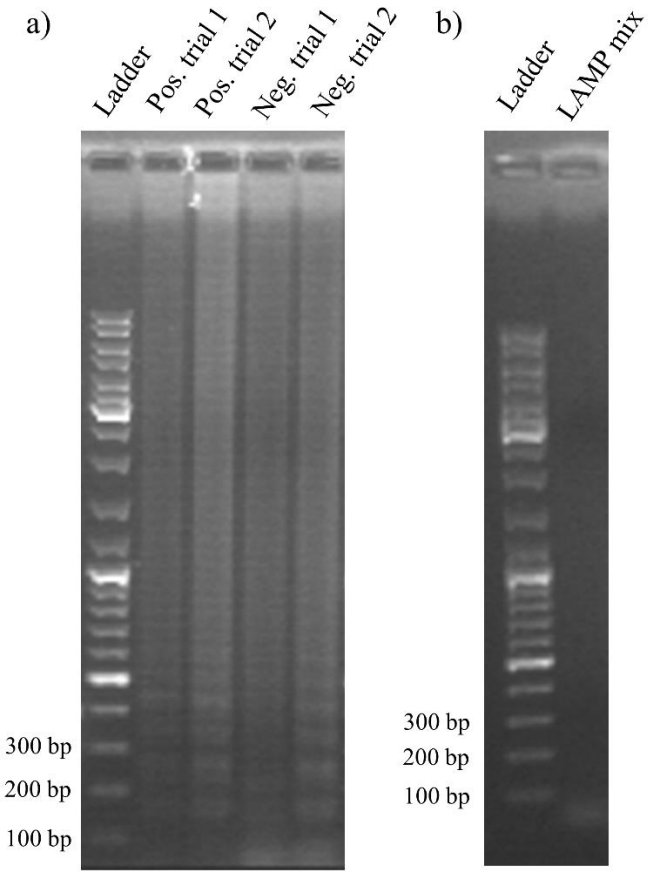

Figure 3.19: Electrophoretic analysis for LAMP on-chip products and reagents, in comparison with a DNA ladder: a) electrophoretic analysis for LAMP on-chip, performed with 65 °C as bottom plate temperature and an initial DNA amount of 10 ng (trial 1) or initial DNA concentration of 0.5 ng/µL (trial 2), for 60 min. and 1.62 µL. b) Electrophoretic analysis for the LAMP master mix.

As can be seen on figure 3.19 a), the temperature increase resulted in more intense bands, as was intended. It is noteworthy that the positive control for trial 2 (maintain initial DNA concentration equal to 0.5 ng/µL) is more intense than the positive control for trial 1 (maintain initial DNA amount equal to 10 ng), suggesting that maintaining DNA concentration yields a more efficient amplification than maintaining the DNA amount. For trial 1, the greater amount of DNA (and consequently, greater DNA concentration) is likely to inhibit the amplification reaction.

Both negative controls present DNA amplification, even after the biological cleaning protocol. According to figure 3.19 b), there are no signs of contamination for the LAMP master mix, which further indicates that the source of contamination is on the chip. One possible explanation for the contamination is primers annealing to each other. When part of a primer sequence is complementary to part of another primer sequence, it is possible that both primers anneal to each other. If this

phenomenon occurs multiple times, the polymerase can interpret the annealed primers as DNA in double-strand, and can start the polymerisation of novel DNA strands. Nevertheless, there is a clear difference in band intensity between positive and negative controls for trial 2, which means that the chip can discriminate between both controls, for the current reaction conditions.

Heretofore, I have demonstrated that the DMF platform can clearly discriminate between a negative and a positive control for 0.5 ng/µL initial DNA concentration, 60 min. reaction time and 65 °C as bottom plate temperature, despite DNA amplification in the negative control. However, for such long reaction times, even by applying reduced voltage at the mixing region during LAMP reactions, the DMF chip itself can undergo some degradation, which may result in LAMP inhibition. As such, in an attempt to preserve the integrity of the devices throughout the entire reaction, an on-chip reaction time study was performed, for 15 min., 30 min. and 45 min., with a bottom-plate temperature of 65 °C and initial DNA concentration of 0.5 ng/µL. Figure 3.20 a) shows the electrophoretic analysis of the LAMP products for the reaction time study.

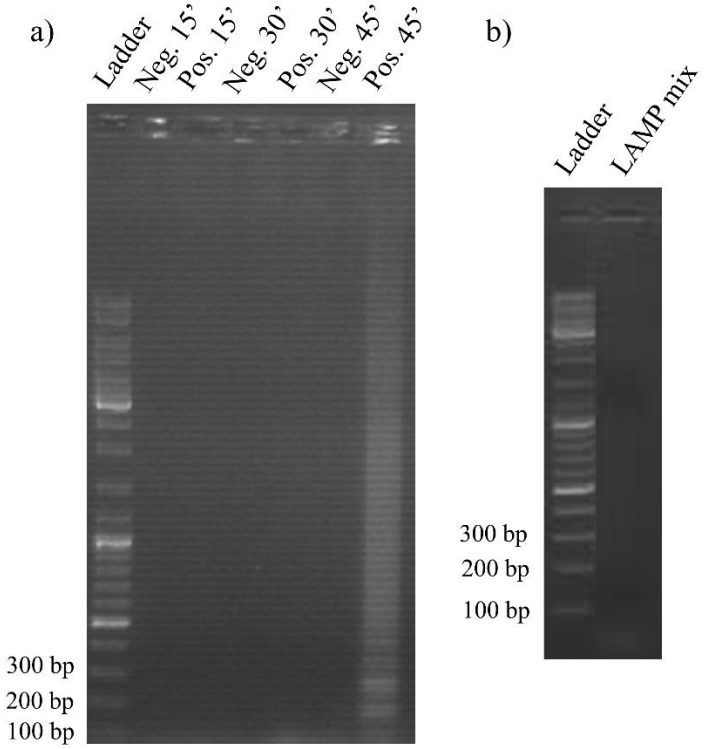

Figure 3.20: Electrophoretic analysis for LAMP on-chip products and reagents, in comparison with a DNA ladder. a) Electrophoretic analysis for LAMP products resulting from an on-device amplification reaction with initial DNA concentration of 0.5 ng/µL and bottom plate temperature of 65 °C. Several reaction times were tested: 15 min., 30 min. and 45 min. b) Electrophoretic analysis for the LAMP master mix.

As can be seen on figure 3.20 a), there was no DNA amplification for 15 min. and 30 min., however, for 45 min., there was DNA amplification for the positive control, but not for the negative control. This means that, for 45 min. reaction time, 65 °C as bottom plate temperature and initial DNA concentration of 0.5 ng/µL, the DMF device is fully capable of distinguishing a negative control from a positive control, which is a remarkable accomplishment. The LAMP mix was also free of visible contamination, as can be seen on figure 3.20 b). It is curious to notice that the amplification products for the above-mentioned conditions produce a brighter band than the amplification products for the same reaction time and initial DNA concentration, at 65 °C, for the bench-top reaction (see section 3.2.1), which suggests that the on-chip LAMP reaction is more efficient than the bench-top reaction.

I thus demonstrate that, for the above-mentioned conditions, a DMF platform may be used to effectively detect 0.5 ng/µL of the target *c-Myc* DNA in just 1.62 µL, one of the lowest volumes ever tested on microfluidic platforms for DNA amplification[34–38,40–42,44].

4. Conclusions and Future Perspectives

Digital Microfluidics is one of the most promising technologies for liquid manipulation, since droplets with volumes ranging from pico- to micro- scale can be independently addressed by an electrode array. As a result, incredibly small reactors are created, where a variety of reactions may occur, from a wide range of scientific areas, such as Biology, Medicine or Chemistry. On the other hand, Loop-mediated Isothermal Amplification has recently emerged as a valid competitor to the most used nucleic acid amplification technology, Polymerase Chain Reaction, mainly due to its simplicity and isothermal character. Joining such promising techniques in a single platform would result in a novel, innovative approach to lab-on-chip applications and point-of-care diagnostics.

In this work, I present the first DMF platform for LAMP amplification of nucleic acids, namely a fragment of the *c-Myc* proto-oncogene, which is overexpressed in about 40% of all known cancers.

First of all, the *c-Myc* amplification by LAMP was thoroughly studied by standard bench-top methods, in order to understand exactly the limits and capabilities of this particular reaction. This initial study also aimed to identify possible amplification conditions for the DMF platform, which would ideally yield efficient amplification of the target DNA: 65 °C as reaction temperature, 60 min. as reaction time, 2 µL as reaction volume and 0.5 ng/µL as initial DNA concentration. A real-time analysis of the LAMP reaction was also performed, for initial DNA concentrations between 0.5 ng/µL and 0.05 pg/µL (10-fold dilutions), and a general dislocation of the reactions towards later times was verified. This dislocation is most likely due to hindrance from the intercalating dye used as fluorescence agent.

Secondly, a DMF platform was developed and its performance was thoroughly tested. The DMF platform I propose is a two-plate device, where: 1) the bottom plate includes chromium electrodes, covered by Parylene C and Teflon® AF and 2) the top plate includes an ITO ground electrode, covered with a Teflon® AF layer, where ports were drilled, which allow simpler sample inlet/outlet, by using a mere pipette. I also propose two different electrode configurations: a "standard" configuration with squared electrodes and a novel configuration with full and half zig-zag shaped electrodes. All fluidic operations (dispensing, splitting, merging and mixing) are possible for operating conditions of 50 V_{RMS}, at 5 kHz for the standard electrode configuration (configuration A), as well as the novel zig-zag electrode configuration (configuration B). Droplet motion was also found to be possible for extremely low operating voltages (12 V_{RMS}) for both configurations. Maximum and minimum droplet velocities were also determined, ranging from (0.25 ± 0.03) mm/s (60 V_{RMS}) to (2.0 ± 0.2) µm/s (12V_{RMS}) for square electrodes, and (0.22 ± 0.02) mm/s (60 V_{RMS}) to (2.4 ± 0.2) µm/s (12V_{RMS}) for zig-zag electrodes. For most of the operating voltages tested, squared electrodes were proven to yield higher droplet velocities than zig-zag electrodes, yet for lower voltages (below 17 V_{RMS}) there seems to be an inversion of this tendency, and zig-zag electrodes yield slightly higher droplet velocities. Nevertheless, droplet velocities were lower than the ones described in the literature, which is possibly due to the fact that the silicone oil used in this work presents a relatively high viscosity, whereas low viscosity oil fillers are preferred in DMF.

The dielectric behaviour of Parylene C with frequency was also evaluated, and a low frequency dielectric relaxation was identified. This dielectric relaxation is presented as a broad peak in the loss tangent, and as a significant decrease in relative permittivity for low frequencies. However, the relaxation frequency is much lower than the working frequency range of the device (around 5 kHz). The Parylene C dielectric constant was also determined, from MIM-like structures with Parylene C as an insulator, and it was found that the dielectric constant is consistent with the literature value (3.07 and 3.00, respectively, at this frequency and room temperature).

The temperature control system was also tested, since temperature control is of great importance in a LAMP reaction (the optimum temperature range for the *Bst* polymerase is between 60 °C and 65 °C). Briefly, temperature generated in the bottom plate is quickly transferred to the rest of the chip, and even though there is a small overshoot on the bottom plate, when temperature surpasses the setpoint, this overshoot does not diffuse to the top plate due to thermal inertia, and therefore no significant

temperature variations occur during a LAMP reaction. The PID controller also functions correctly, given that temperature at the bottom plate is kept quite stable. However, due to the system configuration, the temperature at the bottom plate differs from the temperature at the top plate, and reaction droplets may suffer a temperature gradient around 0.5 °C. As such, the bottom plate temperature should be kept at 65 °C, in order to guarantee that, even with a certain temperature gradient across a reaction droplet, LAMP occurs within optimal temperature range.

Finally, LAMP reactions were performed on-chip. Since LAMP had never been performed on a DMF platform, two hypotheses were initially posited: 1) maintain the initial DNA amount (10 ng) and 2) maintain the initial DNA concentration (0.5 ng/µL). The first hypothesis was firstly tested for 60 min., with a bottom plate temperature of 63 °C, yielding a droplet temperature closer to 60 °C, in a last attempt to lower the reaction temperature and therefore reduce energy consumption. Amplification was successful, yet the electrophoretic analysis revealed dim bands for the positive control, suggesting low amplification efficiency. Furthermore, DNA amplification was also visible in the negative control, suggesting device contamination. As such, a biological cleaning protocol was implemented, and the same hypothesis was tested for 65 °C as bottom plate temperature, for 60 min., achieving a higher amplification efficiency. The second hypothesis was also tested, for the same reaction conditions. Amplification was also possible in this case, with higher efficiency than all the previously tested conditions. Thus, the DMF device does allow a clear distinction between negative and positive controls.

Furthermore, in an attempt to prevent device degradation throughout a LAMP reaction, a reaction time study was performed, for 15 min., 30 min. and 45 min. As a result, amplification was possible for 45 min., with no visible signs of contamination. This DMF platform is thus capable of effectively detecting 0.5 ng/µL of the target *c-Myc* DNA in just 1.62 µL and 45 min. reaction time.

Nevertheless, there is always room for improvements, especially when diagnostics are involved. In order to completely overcome the possibility of contamination in successive on-chip LAMP reactions, the best approach would be to fabricate disposable devices, which may only be used once. Thus, cross contamination from subsequent LAMP reactions with different DNA samples would be prevented. Even though the developed chips yield successful LAMP reactions, low viscosity oil should also be tested as medium filler, in order to further hasten the on-chip LAMP process.

Another interesting future development would be real-time reaction detection, which could be achieved in two ways: 1) a fluorimeter could be integrated into the system, in order to detect fluorescent dyes, such as EvaGreen, which would have to be added to the LAMP reagents, thus allowing the same kind of real-time LAMP detection as with the bench-top equipment and 2) impedance measurements could be integrated into the device, which would only require linking an impedance analyser to the system, thus allowing real-time reaction follow-up with a novel and innovative system. Finally, the present DMF platform is only capable of a small part of the applications enabled by this novel technology. Future DMF systems for nucleic acid amplification would include several DNA targets, which could be amplified and detected simultaneously, with lower reaction volumes, lower cost and lower energy requirements, comparing to conventional LAMP amplification.

References

1. Choi K, Ng AHC, Fobel R, Wheeler AR. Digital Microfluidics. *Annu Rev Anal Chem*. 2012;5(1):413-440. doi:10.1146/annurev-anchem-062011-143028.

2. Jebrail MJ, Bartsch MS, Patel KD. Digital microfluidics: a versatile tool for applications in chemistry, biology and medicine. *Lab Chip*. 2012;12(14):2452. doi:10.1039/c2lc40318h.

3. Pollack MG, Pamula VK, Srinivasan V, Eckhardt AE. Applications of electrowetting-based digital microfluidics in clinical diagnostics. *Expert Rev Mol Diagn*. 2011;11(4):393-407. doi:10.1586/erm.11.22.

4. Samiei E, Tabrizian M, Hoorfar M. *A Review of Digital Microfluidics as Portable Platforms for Lab-on a-Chip Applications*. Quebec; 2016. doi:10.1039/C6LC00387G.

5. Futrell K. *The Future Outlook for Laboratory Point-of-Care Testing*. Carmel, Indiana; 2015.

6. Markets and Markets. Point-of-Care Diagnostics Market by Products (Glucose, Cardiometabolic Monitoring, & Infectious Disease Testing Kits, Cardiac & Tumor Markers), End Users (Home, Hospitals, Ambulatory Care), Over-the- Counter & Prescription Based - Global Forecast to 2021. 2016. http://www.marketsandmarkets.com/Market-Reports/point-of-care-diagnostic-market-106829185.html. Accessed June 20, 2016.

7. Global Industry Analysts Inc. Genetic Testing Market Trends. 2015. http://www.strategyr.com/MarketResearch/Genetic_Testing_Market_Trends.asp. Accessed June 20, 2016.

8. Miller DM, Thomas SDS, Islam A, Muench D, Sedoris K. c-Myc and Cancer Metabolism. *Clin Cancer Res*. 2012;18(20):5546-5553. doi:10.1158/1078-0432.CCR-12-0977.

9. Dang C V. MYC, metabolism, cell growth, and tumorigenesis. *Cold Spring Harb Perspect Biol*. 2013;5(8):1-16. doi:10.1101/cshperspect.a014217.

10. Berthier J. *Micro-Drops and Digital Microfluidics*.Ed. 2. Waltham: Elsevier Inc.; 2013.

11. Millington DS, Sista R, Eckhardt A, et al. Digital Microfluidics: A Future Technology in the Newborn Screening Laboratory? *Semin Perinatol*. 2010;34(2):163-169. doi:10.1053/j.semperi.2009.12.008.

12. Jebrail MJ, Wheeler AR. Let's get digital: digitizing chemical biology with microfluidics. *Curr Opin Chem Biol*. 2010;14(5):574-581. doi:10.1016/j.cbpa.2010.06.187.

13. García AA, Egatz-Gómez A, Lindsay SA, et al. Magnetic movement of biological fluid droplets. *J Magn Magn Mater*. 2007;311(1):238-243. doi:10.1016/j.jmmm.2006.10.1149.

14. Darhuber A, Valentino JP, Troian SM. Planar digital nanoliter dispensing system based on thermocapillary actuation. *Lab Chip*. 2010;10(8):1061-1071. doi:10.1039/b921759b.

15. Chiou PY, Park SY, Wu MC. Continuous optoelectrowetting for picoliter droplet manipulation. *Appl Phys Lett*. 2008;93(22):22-24. doi:10.1063/1.3039070.

16. Park S-Y, Teitell M, Chiou EPY. Single-sided continuous optoelectrowetting (SCOEW) for droplet manipulation with light patterns. *Lab Chip*. 2010;10(13):1655-1661. doi:10.1039/c001324b.

17. Guttenberg Z, Mu H, Habermu H, Geisbauer A, Felbel J, Kielpinski M. Planar chip device for PCR and hybridization with surface acoustic wave pump. *Lab Chip*. 2005;5(3):308-317. doi:10.1039/b412712a.

18. Pesant J, Hareng M, Mourey B, Perbet J. Electrodes for a device operating by electrically

controlled fluid displacement. 1986.

19. Pollack MG, Fair RB, Shenderov AD. Electrowetting-based actuation of liquid droplets for microfluidic applications. *Appl Phys Lett*. 2000;77(11):1725. doi:10.1063/1.1308534.

20. Lee J, Moon H, Fowler J, Schoellhammer T, Kim C-J. Electrowetting and electrowetting-on-dielectric for microscale liquid handling. *Sensors Actuators A Phys*. 2002;95(2-3):259-268. doi:10.1016/S0924-4247(01)00734-8.

21. Cho SK, Moon H, Kim CJ. Creating, transporting, cutting, and merging liquid droplets by electrowetting-based actuation for digital microfluidic circuits. *J Microelectromechanical Syst*. 2003;12(1):70-80. doi:10.1109/JMEMS.2002.807467.

22. Sista R, Hua Z, Thwar P, et al. Development of a digital microfluidic platform for point of care testing. *Lab Chip*. 2008;8(12):2091-2104. doi:10.1039/b814922d.

23. Abdelgawad M, Freire SLS, Yang H, Wheeler AR. All-terrain droplet actuation. *Lab Chip*. 2008;8(5):672. doi:10.1039/b801516c.

24. Nelson WC, Kim C-J "Cj." Droplet Actuation by Electrowetting-on-Dielectric (EWOD): A Review. *J Adhes Sci Technol*. 2012;26:1747-1771. doi:10.1163/156856111X599562.

25. Moon H, Cho SK, Garrell RL, Kim C-J "Cj", Garrell RL. Low voltage electrowetting-on-dielectric. *J Appl Phys*. 2002;92(7):4080-4087. doi:10.1063/1.1504171.

26. Quilliet C, Berge B. Electrowetting: A recent outbreak. *Curr Opin Colloid Interface Sci*. 2001;6(1):34-39. doi:10.1016/S1359-0294(00)00085-6.

27. Jebrail MJ, Sinha A, Vellucci S, et al. World-to-Digital-Microfluidic Interface Enabling Extraction and Purification of RNA from Human Whole Blood. *Anal Chem*. 2014;86(8):3856-3862. doi:10.1021/ac404085p.

28. Welch ERF, Lin YY, Madison A, Fair RB. Picoliter DNA sequencing chemistry on an electrowetting-based digital microfluidic platform. *Biotechnol J*. 2011;6(3):165-176. doi:10.1002/biot.201000324.

29. Malic L, Veres T, Tabrizian M. Biochip functionalization using electrowetting-on-dielectric digital microfluidics for surface plasmon resonance imaging detection of DNA hybridization. *Biosens Bioelectron*. 2009;24(7):2218-2224. doi:10.1016/j.bios.2008.11.031.

30. Nolan T, Bustin S. *PCR Technology: Current Innovations*. Ed. 3. Boca Raton: CRC Press; 2013. doi:10.1201/b14930-30.

31. Kleppe K, Ohtsuka E, Kleppe R, Molineux I, Khorana H. Studies on Polynucleotides XCVI. Repair Replication of Short Synthetic DNA's as catalyzed by DNA polymerases. *J Mol Biol*. 1971;56:341-361. doi:10.1016/0022-2836(71)90469-4.

32. Mullis K, Faloona F, Scharf S, Saiki R, Horn G, Erlich H. Specific Enzymatic Amplification of DNA In Vitro: The Polymerase Chain Reaction. *Cold Spring Harb Symp Quant Biol*. 1986;51:263-273. doi:10.1234/12345678.

33. Gill P, Ghaemi A. Nucleic Acid Isothermal Amplification Technologies — A Review. *Nucleosides, Nucleotides, and Nucleic Acids*. 2008;27(3):224-243. doi:10.1080/15257770701845204.

34. Chang YH, Lee GB, Huang FC, Chen YY, Lin JL. Integrated polymerase chain reaction chips utilizing digital microfluidics. *Biomed Microdevices*. 2006;8(3):215-225. doi:10.1007/s10544-006-8171-y.

35. Hua Z, Rouse JL, Eckhardt AE, et al. Multiplexed real-time polymerase chain reaction on a digital microfluidic platform. *Anal Chem*. 2010;82(6):2310-2316. doi:10.1021/ac902510u.

36. Fouillet Y, Jary D, Brachet A, et al. EWOD digital microfluidics for Lab on a Chip. In: The American Society of Mechanical Engineers, ed. *ASME 4th International Conference on Nanochannels, Microchannels and Minichannels*. Limerick: ASME Press; 2006:1255-1264. doi:0-7918-4760-8.

37. Berthier J, Mourier V, Sarrut N, et al. Some examples of micro-devices for biotechnology developed at the Department of Technologies for Life Sciences and Healthcare of the LETI. *Int J Nanotechnol*. 2010;7(4-8):802-818. doi:10.1504/IJNT.2010.031745.

38. Ugsornrat K, Afzulpurkar N V, Wisitsoraat A, Tuantranont A. Design, Simulation, and Experimental Study of a Droplet-Based PCR by EWOD. *Sensors Mater*. 2010;22(6):271-284.

39. Ugsornrat K, Maturus T, Jomphoak A, et al. Simulation and Experimental Study of Electrowetting on Dielectric (EWOD) Device for a Droplet Based Polymerase Chain Reaction System. In: Teck L, Hong J, eds. *IFMBE Proceedings: Multidisciplinary Studies of Mechanical Engineering, Electrical Engineering and Biological Sciences and Its Application to Solve Medical Problems*. Singapore: Springer; 2009:859-862. doi:978-3-540-92841-6.

40. Norian HS, Shepard K, Kymissis J, Field R. An integrated CMOS quantitative-polymerase-chain-reaction lab-on-chip for point-of-care diagnostics. *Lab Chip*. 2014;14(20):4076-4084. doi:10.1039/C4LC00443D.

41. Kalsi S, Valiadi M, Tsaloglou M, et al. Rapid and sensitive detection of antibiotic resistance on a programmable digital microfluidic platform. *Lab Chip*. 2015;15(14):3065-3075. doi:10.1039/C5LC00462D.

42. Kühnemund M, Witters D, Nilsson M, Lammertyn J. Circle-to-circle amplification on a digital microfluidic chip for amplified single molecule detection. *Lab Chip*. 2014;14(16):2983-2992. doi:10.1039/C4LC00348A.

43. Notomi T, Okayama H, Masubuchi H, et al. Loop-mediated isothermal amplification of DNA. *Nucleic Acids Res*. 2000;28(12):e63. doi:10.1093/nar/28.12.e63.

44. Chang C-M, Chang W-H, Wang C-H, Wang J-H, Mai J, Lee G-B. Nucleic acid amplification using microfluidic systems. *Lab Chip*. 2013;13(7):1225-1242. doi:10.1039/c3lc41097h.

45. Notomi T, Mori Y, Tomita N, Kanda H. Loop-mediated isothermal amplification (LAMP): principle, features, and future prospects. *J Microbiol*. 2015;53(1):1-5. doi:10.1007/s12275-015-4656-9.

46. Eiken Chemical Co. L. The principle of LAMP method - Basic principle. 2005. http://loopamp.eiken.co.jp/e/lamp/principle.html. Accessed July 15, 2016.

47. Ahmad F, Seyrig G, Tourlousse DM, Stedtfeld RD, Tiedje JM, Hashsham SA. A CCD-based fluorescence imaging system for real-time loop-mediated isothermal amplification-based rapid and sensitive detection of waterborne pathogens on microchips. *Biomed Microdevices*. 2011;13(5):929-937. doi:10.1007/s10544-011-9562-2.

48. Wang C-H, Lien K-Y, Wu J-J, Lee G-B. A magnetic bead-based assay for the rapid detection of methicillin-resistant Staphylococcus aureus by using a microfluidic system with integrated loop-mediated isothermal amplification. *Lab Chip*. 2011;11(8):1521-1531. doi:10.1039/c0lc00430h.

49. Stedtfeld RD, Tourlousse DM, Seyrig G, et al. Gene-Z: a device for point of care genetic testing using a smartphone. *Lab Chip*. 2012;12(8):1454. doi:10.1039/c2lc21226a.

50. Fobel R, Fobel C, Wheeler AR. DropBot: An open-source digital microfluidic control system with precise control of electrostatic driving force and instantaneous drop velocity measurement. *Appl Phys Lett*. 2013;102(19):1-5. doi:10.1063/1.4807118.

51. Chang TY, Yadav VG, De Leo S, et al. Cell and protein compatibility of parylene-C surfaces. *Langmuir*. 2007;23(23):11718-11725. doi:10.1021/la7017049.

52. Kahouli A, Sylvestre A, Ortega L, et al. Structural and dielectric study of parylene C thin films. *Appl Phys Lett*. 2009;94(15):152901. doi:10.1063/1.3114404.

53. Speciality Coating Systems. SCS Parylene Properties. *Parylene Knowl*. 2014. http://scscoatings.com/what-is-parylene/parylene-properties/. Accessed July 19, 2016.

54. Rodrigues V. [MSc thesis] Digital Microfluidic devices : the role of the dielectric layer, Faculdade de Ciências e Tecnologia - Universidade Nova de Lisboa, 2014.

55. Shackelford J, Han Y-H, Kim S, Kwon S-H. *CRC Materials Science and Engineering Handbook*. Vol Fourth Edi. Boca Raton: CRC Press; 2016.

56. Pollack MG. [PhD thesis] Electrowetting-based microactuation of droplets for digital microfluidics, University of Duke, 2001.

57. Nagamine K, Hase T, Notomi T. Accelerated reaction by loop-mediated isothermal amplification using loop primers. *Mol Cell Probes*. 2002;16(3):223-229. doi:10.1006/mcpr.2002.0415.

58. Fang X, Chen H, Xu L, Jiang X, Wu W, Kong J. A portable and integrated nucleic acid amplification microfluidic chip for identifying bacteria. *Lab Chip*. 2012;12(8):1495. doi:10.1039/c2lc40055c.

59. Meixeiro C. *Optimization of the Direct Stochastic Optical Reconstruction Microscopy (dSTORM) of the Unidade de Imagiologia Celular of Instituto Gulbenkian de Ciência*. Lisbon; 2016.

60. Soares M. [MSc thesis] Control System for Actuation and Sensing in Digital Microfluidics Devices, Faculdade de Ciências e Tecnologia - Universidade Nova de Lisboa, 2014.

Annex 1 – Comparison between DMF platforms for nucleic acid amplification

Table A1.1 presents a short comparison between the existing DMF platforms for nucleic acid amplification, to this date.

Table A1.1: A comparative study of the existing DMF platforms for nucleic acid amplification to date.

		Author						
	Parameter	Norian *et al.*[40]	Kalsi *et al.*[41]	Ugsornrat *et al.*[38]	Fouillet *et al.*[37]	Chang *et al.*[34]	Sista *et al.*[22]	Hua *et al.*[35]
	Dielectric material	Parylene C	Ion barrier insulator (Al_2O_3)	Silicon dioxide (SiO_2)	Silicon nitride (Si_3N_4)	Silicon nitride (Si_3N_4)	-	-
	Dielectric thickness	2 µm	300 nm	100 nm	3000 Å	0.15 µm	-	-
	Hydrophobic layer material	Teflon® AF	Cytop®	Teflon® AF	Teflon® AF	Teflon® AF	-	-
	Hydrophobic layer thickness	100 nm	80 nm	20 nm	A few hundred nm	0.05 µm	-	-
	Electrode material	-	ITO	Chromium/Gold (Cr/Au)	Gold	Gold	-	-
	Electrode thickness	-	-	100 nm	3000 Å	0.12 µm	-	-
	Electrode area	200x200 µm	200x200 µm	-	800x800 µm	1.38x1.38 mm	1.125x1.125 mm (pitch)	1.1x1.1 mm
	Gap between electrodes	-	10 µm	-	-	20 µm	-	-
	Ground electrode material	ITO+PEN	ITO	ITO	ITO (polycarbonate plate)	ITO	ITO	ITO
	Substrate material	-	Glass	Glass	Glass	Glass	PCB	PCB
	Gap between plates	100 µm	125 µm (Mylar spacer)	250 µm (PDMS channel defines the spacing)	100 µm (Ordyl spacer)	370 µm (JSR-50 photoresist spacer)	185 µm	275 µm
	Filler	n-dodecane	n-dodecane	Silicone oil	Silicone oil	Silicone oil	Hexadecane	Hexadecane/ silicone oil
	Actuation voltage	90 V (70 V to 250 V)	20 V	-	60 V_{RMS} (3 kHz)	12 V_{RMS} (3 kHz)	12 V_{RMS}	-
	Sealing	Yes, SU-8	-	Yes, PDMS channel	Yes, Ordyl	-	Yes, polymer film	Yes, polymer film
	Chip dimensions	4x4 mm	7.37 cm^2	-	13x13 mm	6.5x4.5 cm	8.55x12.78 cm	86x86 mm
	Droplet volume	1.2 nL	45 nL	-	64 nL	730 nL	300 nL	330 nL
	Amplification technique	PCR	PCR	PCR	PCR	PCR	PCR	PCR

Annex 2 – Comparison between PCR and LAMP

Table A2.1 compares the main aspects of both PCR and LAMP amplification techniques.

Table A2.1: Main characteristics of PCR and LAMP amplification methods.

	PCR	LAMP
Possible templates	DNA, RNA[44]	DNA, RNA[44]
Resulting amplicon	Double-stranded DNA[44]	Concatenated DNA[44]
By-products	Few (mostly primer dimers)	Many[43]
Required temperature	3 different cycling temperatures: 95 °C, 50 °C - 65 °C, 72 °C[32]	60 °C - 65 °C[43]
Number of primers required	2[32]	4 - 6[57]
Number of enzymes required	1 (*Taq* polymerase)[32]	1 (*Bst* polymerase)[43]
Denaturation required	Yes[32]	No[44]
Sensitivity	10^1-10^2 target strands[44]	1 target strand[44]
Amplification factor and reaction time	Approximately 2^{30}-fold in 2 to 3 hours[44]	10^9 fold in 1 hour[44]
Tolerance to biological elements which do not belong to the reaction	Low[58]	High[58]

Annex 3 – Plasmid DNA extraction by alkaline lysis protocol

Prior to DNA extraction itself, 500 mL of LB medium were prepared as follows: 1) dissolve 5 g of bacto-tryptone (BDH Chemicals), 2.5 g of bacto-yeast extract (Fluka) and 5 g of NaCl (Sigma-Aldrich) into 475 mL of deionized water; 2) adjust the solution pH to 7.0, by adding the necessary drops of a 5 M NaOH solution; 3) adjust the final solution volume to 500 mL with deionized water and 4) sterilise the solution by autoclaving and store at 4 °C.

In order to perform the alkaline lysis procedure, the following solutions were prepared:

- Lysis I: 50 mM glucose (Sigma-Aldrich), 25 mM Tris.HCl (Sigma-Aldrich) at pH 8.0 and 10 mM EDTA (Fluka) at pH 8.0;
- Lysis II: 0.2 M NaOH and 1% (wt/v) SDS;
- Lysis III: 60 mL of a 5 M potassium acetate solution, 11.5 mL of glacial acetic acid and 28.5 mL of deionized water.

Succeeding *E.coli* incubation, the resulting volume was divided into 1.5 mL partitions and alkaline lysis was performed according to the following steps:

- The bacteria were precipitated by centrifugation at 10 krpm, 4 °C for 5 min. and the supernatant was discarded. 150 µL of lysis I were added to each partition, mixed by inversion and cooled on ice for 5 min.;
- After cooling, 300 µL of lysis II were added to each partition, and the resulting solution was then mixed by inversion, to which followed cooling on ice for another 5 min.;
- 25 µL of lysis III were then added, mixed by inversion and cooled on ice for 20 min.;
- After cooling, the resulting solution was centrifuged at 13 krpm, 4 °C for 20 min. and all the supernatant was recovered and placed into new sterile tubes;
- 2 volumes of absolute ethanol (4 °C) were added and the solution was placed at -20 °C for 2 hours;
- The solution was then centrifuged at 13 krpm, 4 °C for 20 min. and the majority of the supernatant was discarded;
- The remaining supernatant was dried in vacuum (SpeedVac Concentrator, Savant) for 5 min.
- The precipitates of half the tubes were dissolved in 200 µL of pure water, which resulted in 2 tubes of 200 µL, each containing half of the total extracted DNA;
- 4 µL of RNAseA (1:50 proportion) were added to each tube and enzyme digestion occurred for 3 hours;
- 300 µL of pure water were added to each tube, to attain a final volume of 500 µL;
- 500 µL (1 volume) of phenol were added to each tube and mixed by vortex;
- The tubes were centrifuged for 3 min., at 13 krpm;
- The supernatant was recovered and placed in new sterile tubes. To each tube, 500 µL (1 volume) of a chloroform/isoamyl alcohol solution (24:1 v/v proportion) were added and mixed by vortex;
- The solution was centrifuged at 13 krpm, 4 °C for 3 min. and the supernatant was recovered;
- 1 mL (2 volumes) of absolute ethanol (4 °C) was added to each tube and the mix was cooled at -20 °C for 2 hours;
- The solution was centrifuged at 13 krpm, 4 °C for 3 min. and stored at -20 °C overnight before using.

Annex 4 – Loop-mediated Isothermal Amplification reagents and target DNA

All LAMP reactions were performed according to the procedure described by Notomi *et al* [43], in a total reaction volume of 20 µL. The only difference between the protocol used in this work and the one described by Notomi *et al*.[43] is the use of magnesium chloride ($MgCl_2$) instead of magnesium sulphate ($MgSO_4$). Reagents and corresponding concentrations are described in table A4.1.

Table A4.1: LAMP reagents and respective concentrations on LAMP reactions.

Reagents	Concentrations
dNTPs (Fermentas)	400 µM each
FIP (StabVida)	0.8 µM
BIP (StabVida)	0.8 µM
F3 (StabVida)	0.2 µM
B3 (StabBida)	0.2 µM
Betaine (Sigma-Aldrich)	1 M
$MgCl_2$ (Sigma-Aldrich)	4 mM
Enzyme Buffer (New England Biolabs)	1x
Bst Polymerase (New England Biolabs)	0.32 U/µL

The DNA target sequence is a fragment from the human *c-Myc* (ac. no. NC_000008.11), which consists of 158 base-pairs, not including the primers, or 229 base-pairs, including the outer primers. The *c-Myc* target fragment is represented below (5'-3'), flanked by the outer priming regions, highlighted in yellow:

TCTGAAGAGGACTTGTTGCGGAAACGACGAGAACAGTTGAAACACAAACTTGAACAGCT
ACGGAACTCTTGTGCGTAAGGAAAAGTAAGGAAAACGATTCCTTCTAACAGAAATGTCCT
GAGCAATCACCTATGAACTTGTTTCAAATGCATGATCAAATGCAACCTCACAACCTTGGC
TGAGTCTTGAGACTGAA

Furthermore, the FIP, BIP, F3 and B3 sequences (5'-3') are as follows:

- FIP: CTTTTCCTTACGCACAAGAGTTCCGGAAACGACGAGAACAGT
- BIP: ACGATTCCTTCTAACAGAAATGTCCCAAGGTTGTGAGGTTGCA
- F3: TCTGAAGAGGACTTGTTGC
- B3: TTCAGTCTCAAGACTCAGC

Annex 5 – Additional device electrode/reservoir configurations

Apart from configurations A and B, devices with other structures were designed and produced (figure A5.1), for a future thorough study on the influence of further reducing on-chip LAMP reaction volumes and different electrode shapes on the final LAMP products.

- Configuration C relies on standard square reservoirs and electrodes. The mixing region is small to accommodate lower volume LAMP reactions, yet has twice the area of the electrodes, as to assure that two droplets may fit;
- Configuration D has larger electrodes, comparing with configuration C, since some authors[21] consider that higher volume droplets are easier to act upon;
- Configuration E has a small mixing region, to test lower volume LAMP reactions, along with the novel zig-zag shaped electrodes.

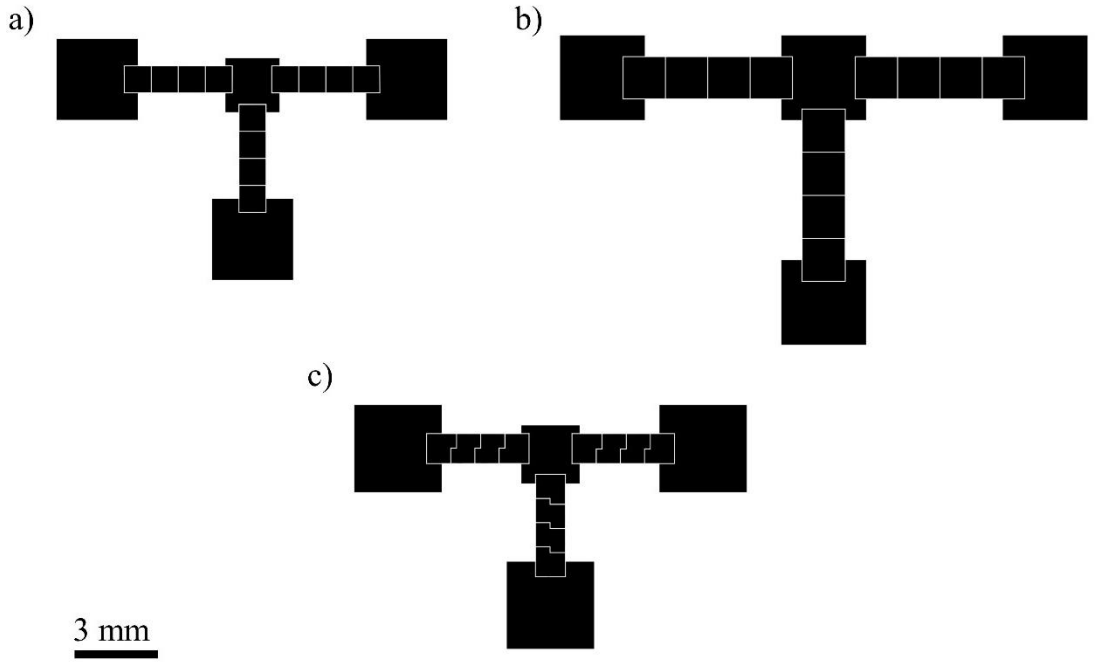

Figure A5.1: Additional device configurations: configuration C (a), configuration D (b) and configuration E (c).

Annex 6 – Heating system

An independent heating system was designed in-house, to provide precise control over the temperature at which LAMP reactions occur. This system was based on the work done by Meixeiro *et al.*[59], and was further adapted and improved for the developed DMF platform. Figure A6.1 shows a schematic of the circuit associated to the ITO thin film resistor, for temperature control.

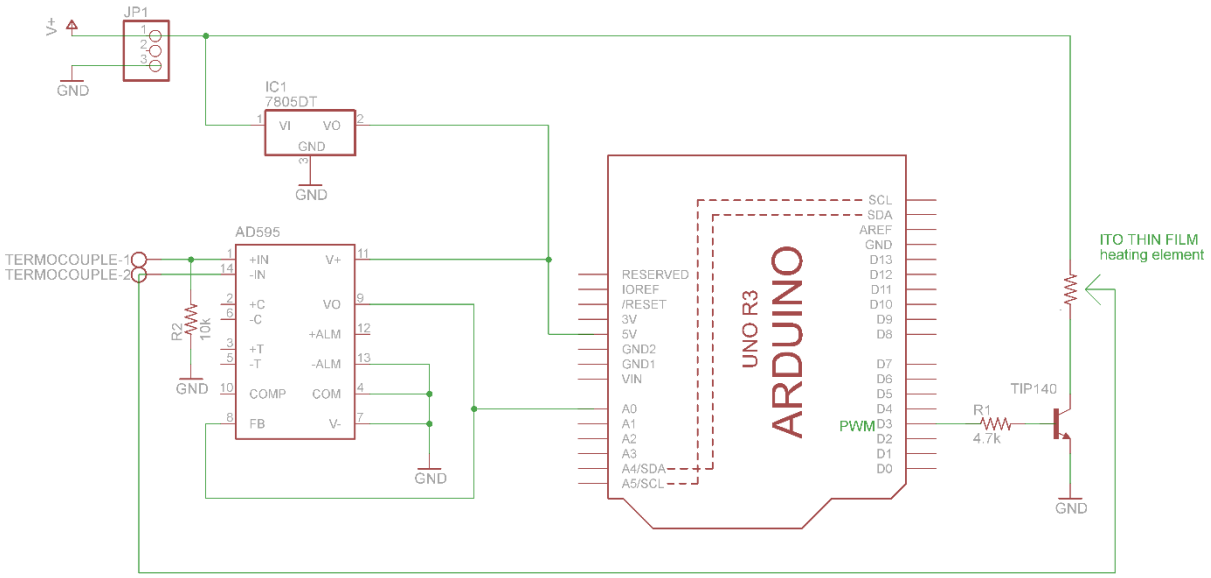

Figure A6.1: Schematic representation of the temperature control system.

Briefly, the power supplied to the ITO thin film is regulated by two different elements: 1) a standard power supply and 2) a power transistor. The power supply provides a constant 9 V voltage drop across the ITO resistor, and the transistor will be responsible for controlling the effective current flowing through the resistor, thus controlling power dissipation as heat at the heating element. The power transistor is connected to an Arduino control board, which in turn is connected to a thermocouple via an AD595 thermocouple amplifier. The thermocouple measures the temperature of the thin film resistor continuously, and through the AD595, information about temperature at the heating element is passed to the Arduino control board. The Arduino board contains a PID software which is constantly comparing the actual temperature of the heating element with the setpoint value (control loop – see figure A6.2). If the temperature is higher/lower than the setpoint, the controller sends a PWM signal to the transistor, which in turn adjusts the current accordingly, to maintain the setpoint temperature. Finally, both the Arduino control board and the AD595 are powered by the same power supply that powers the ITO resistor, however, the signal coming from the power supply is transferred to a voltage regulator that tunes the voltage to 5 V.

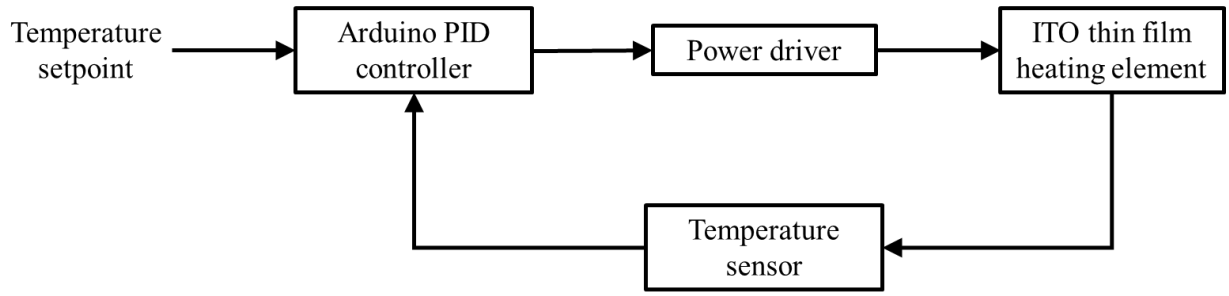

Figure A6.2: Block diagram of the temperature control system, evidencing the continuous loop used to compare the thin film resistor temperature with the setpoint temperature.

Annex 7 – ITO thin film resistor characterisation

As was mentioned earlier in this work, an ITO thin film resistor is responsible for heating the DMF chip, thus providing the necessary temperature for LAMP reactions to occur. Figure A7.1 shows a photograph of the ITO resistor used.

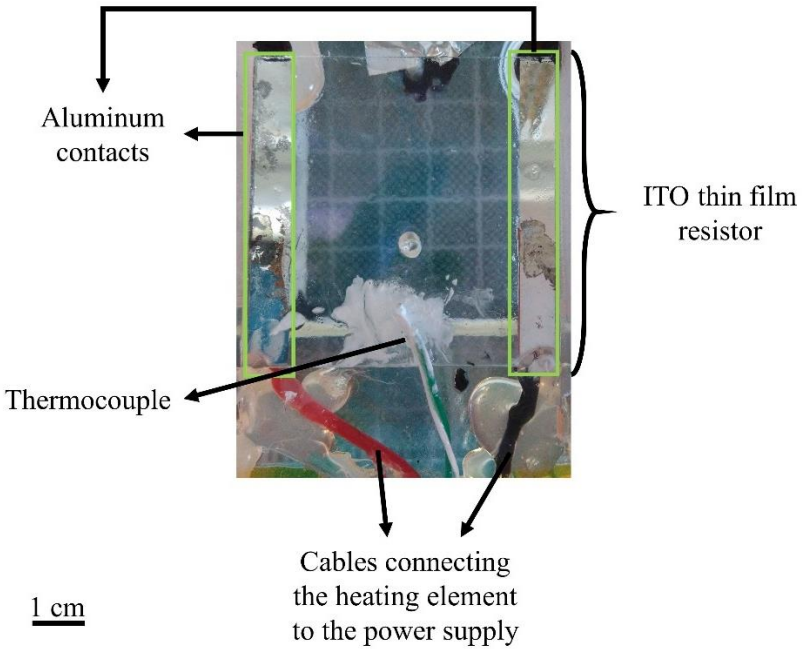

Figure A7.1: Photograph of the ITO thin film resistor used to provide heat for the LAMP reactions, evidencing all the connections to the remaining heating system.

The ITO thin film resistor was well characterised and calibrated, in order to understand the behaviour of the resistance and exactly how much power is necessary to attain a certain temperature. This particular thin film resistor is used as a heating element, thanks to the self-heating phenomenon. Self-heating occurs when current flowing through a conductive material leads to the production of heat, as a consequence of electron collisions with the material lattice. Figure A7.2 shows the behaviour of the heating element in terms of applied current/voltage and dissipated power.

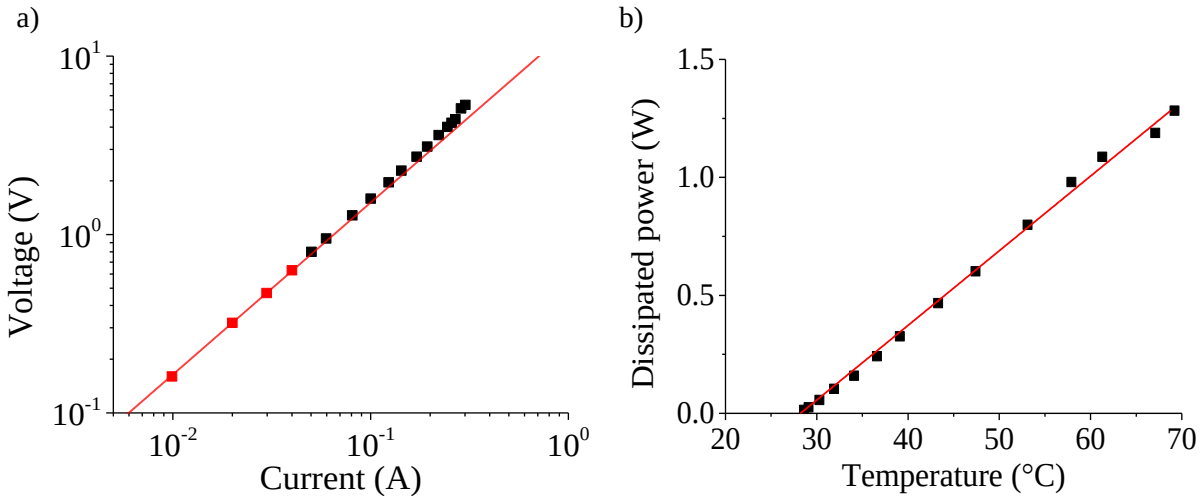

Figure A7.2: a) Voltage supplied to the thermoresistor, as a function of current. The linear fit corresponds to the first data points, represented in red, where linearity between voltage and current is maintained. b) Required power dissipation at the thermoresistor to generate the intended temperatures.

Figure A7.2 a) shows the current flow in the thin film resistor as a function of the applied voltage. For higher current values, the linearity between current and voltage is lost, as can be seen by the deviation of the data points from the linear fit for lower voltage/current data. This is due to the self-heating phenomenon, which increases the effective value of the resistance. It is also clear that temperature rises as a function of the power dissipated at the thermoresistor (figure A7.2 b), as would be expected. To achieve higher temperatures, more power must be dissipated by the thermoresistor, and therefore, more current must be supplied.

Annex 8 – Modelling of Parylene C capacitors, with chromium contacts

As was mentioned in section 3.4.1, several Parylene C capacitors were produced, to evaluate the behaviour of this dielectric with frequency. The capacitors were produced by depositing a (2.20 ± 0.02) µm[**] layer of Parylene C between two crossed layers of chromium contacts, deposited by evaporation with an e-beam equipment, resulting in a MIM-like structure. Figure A8.1 shows the general layout of the capacitors produced.

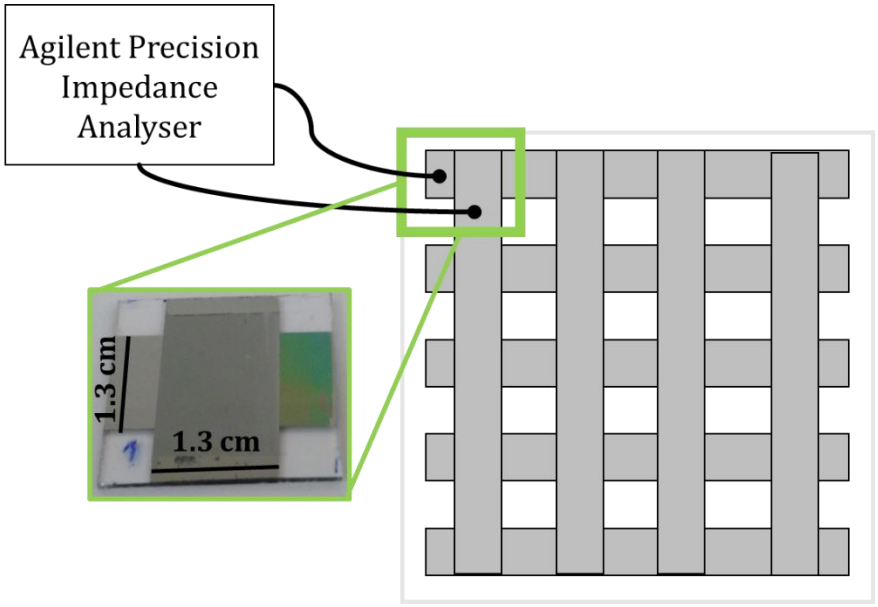

Figure A8.1: Cross-configuration of Parylene C capacitors, evidencing one of the individualised capacitors used to analyse the behaviour of the dielectric material with frequency.

To model the Parylene C capacitors, including both dielectric and contact resistance behaviour, it is necessary to consider a complex capacity, *C**, in series with the contact resistances, as shown in figure 3.11. The complex capacity allows the modelling of the visible broad peak on the loss tangent for low frequencies, which actually corresponds to a Havriliak–Negami dielectric relaxation[52], where the loss tangent peak (over frequency) is much broader than in the case of a Debye relaxation. Moreover, the series resistance allows the modelling of the dominant resistive behaviour for higher frequencies.

A Cole-Cole diagram is particularly helpful for this study, since it may be used to determine the series resistance due to chromium contacts plus test probes. This diagram represents the negative of the impedance imaginary part as a function of the impedance real part (figure A8.2). The impedance for the above-mentioned model is given by equation A8.1:

$$Z = \frac{1}{j\omega C^*} + Rs \tag{A8.1}$$

Where

$$C^* = C' - jC'' \tag{A8.2}$$

Z is the total impedance, *C** is the complex capacitance of the dielectric (*C'* is the real part of the capacitance and *C*'' is the imaginary part), ω is the frequency and *R*s is the contact series resistance.

[**] The uncertainty associated with this thickness was determined based on the maximum deviation from the mean value of 5 measurements (see annex 9).

The value of *R*s can be obtained from the Cole-Cole diagram, by determining the real part of the impedance at high frequencies (intersection of impedance with the real axis). Figure A8.2 shows the Cole-Cole impedance representation.

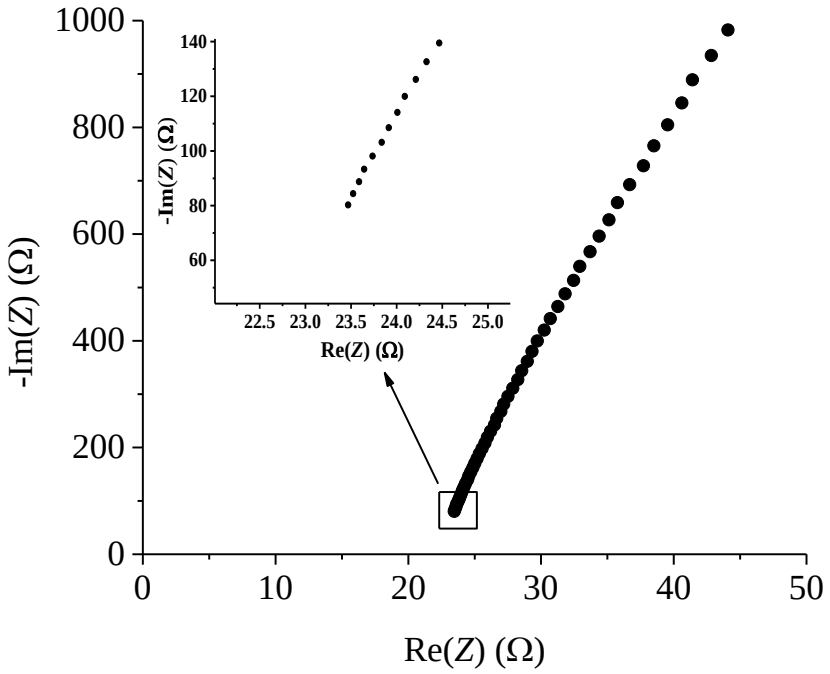

Figure A8.2: Cole-Cole representation of the Parylene C capacitor impedance.

As can be seen on figure A8.2, the series resistance for the model in figure 3.11 is between 22.5 Ω and 23.5 Ω, which is a reasonable value for contact resistance.

Annex 9 – Error determination for material thicknesses

Table A9.1 shows several measurements for material thicknesses, and the associated measuring errors.

Table A9.1: Thickness measurements for several materials, as well as the respective errors.

	Kapton® tape spacer (mm)	Glass (mm)	Parylene C (µm)
	0.176	0.959	2.19
	0.177	0.958	2.21
	0.178	0.960	2.20
	0.176	0.959	2.20
	0.177	0.958	2.18
Mean value	0.177	0.959	2.20
Maximum deviation from mean value (error)	0.001	0.001	0.02

Annex 10 – Arduino and Matlab® software for electrode/reservoir driving

The software required for electrode/reservoir driving was adapted (from 8 to 16 electrodes) and improved for the current DMF platform, from previous work done at CENIMAT[60]. The communication between both the Arduino control board and the computer generates a user-friendly interface that intuitively allows activation/deactivation of every electrode/reservoir. Figure A10.1 represents this interface.

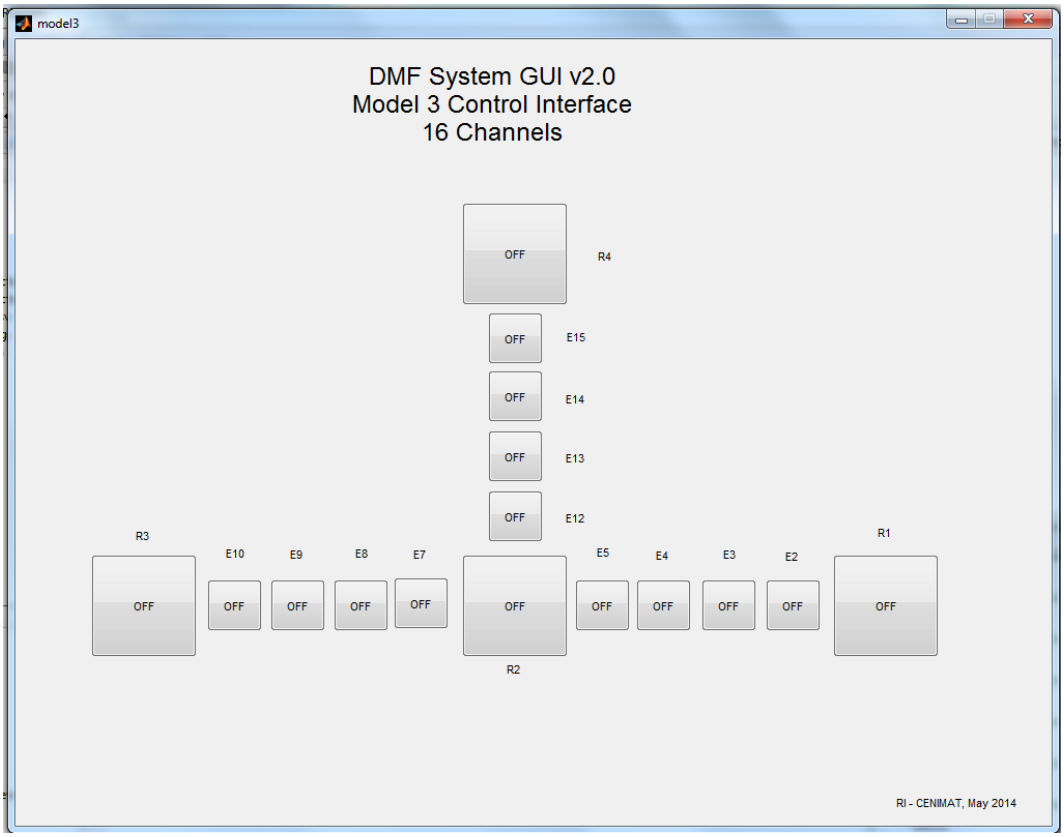

Figure A10.1: Computer-user interface for electrode/reservoir driving.

In this annex, both software codes are described, namely the Arduino code from page 50 to page 53 and the Matlab® code from page 54 to page 61.

Arduino software code

The Arduino software code for electrode control is described below:

```
/*
  DropTempControl
  Reads and control the temperature of a thin film resistor for the DMF setup
  Temperature sensor: type K thermocouple with AD595 cold junction and amplification
  ADC with arduino (10 bits)

  Type K thermocouple with AD595 (Rf=490k ~100mV/C)
  calibrated  against standard laboratory thermocouple system
```

```
  between 30 ºC and 65 ºC
  T = (Tm + 2.6982)/1.07765

  PID controller: output from PWM arduino pin (8bits) and a NPN transistor

  system tested:
  Rload (thin film resistor): 17.5 ohm
  power: NPN Rb=4.7k, Ib=0.9mA, Vcc=9V, Ic=159mA, dV=8.3, Pmax=4130 mW

  The Temperature value is send to the serial port (can be read in matlab)

  Rui Igreja - Set2016 - rev 3
*/
// include the library code:
#include <LiquidCrystal.h>
LiquidCrystal lcd(12, 11, 5, 4, 3, 2); // initialize the library with the numbers of the interface pins
#include <SoftwareSerial.h>

const int sensorPin = A5;          // select the input pin for the sensor
const int outPin = 9;              // output pwm pin
const int buttonUpPin = 6;         // the pin for the pushbutton to increase setpoint
const int buttonDownPin = 7;       // the pin for the pushbutton to decrease setpoint
const int lcdInfo = 1;             //type of information on lcd 1-output; 2-PID parameters

const float LSBvalue = 5.0/1024.0;  // LSB value in Volts (analog scale 5V, ADC 10 bits)

const float m = 1.07765;           // slope from thermocouple calibration
const float b = -2.6982;           // intercept from thermocouple calibration

int buttonStateUp = 0;             // current state of the button to increase setup
int buttonStateDown = 0;           // current state of the button to decrease setup
int nSamples;                      // number of temperature readings to average

float sensorValue;                 // variable to store the value from the sensor reading
float actualTime, lastTime, dt;    // variables for time
float Out, setPoint;               // variables for output and setpoint
float error, derror, lastError;    // variables for the error
float P, I, D, Kp, Ki, Kd;         // variables for the PID controller
float AD595gain;                   // AD595 gain in V/ºC
float Pmax;                        // Maximum power delivery to the load (mW) (for Out=255)

void setup() {

  // set the lcd columns and lines
  lcd.begin(16, 2);

  // initial message
  lcd.setCursor(0, 0);
  lcd.print("DMF Temperature");
  lcd.setCursor(0, 1);
  lcd.print("CENIMAT 09/16 r3");
  delay(2000);
  lcd.clear();

  // set pin modes
```

```
  pinMode(outPin, OUTPUT);
  pinMode(buttonUpPin, INPUT);
  pinMode(buttonDownPin, INPUT);

  // initialize all variables
  actualTime = 0; lastTime = 0;
  dt = 0; Out =0; error=0, derror=0, lastError=0;
  sensorValue = 0;

  // number of readings for each sensor measurement
  nSamples = 250;

  // AD595 chip gain in V/ºC
  AD595gain = 0.0594;

  // Maximum power in load (mW) (for out=255)
  Pmax=4.130;

  // initial parameters for setPoint and PID constants
  setPoint = 23.0;
  Kp=75.0; Ki=1; Kd=15;

  // Serial communication initiation
  Serial.begin(9600);

} //setup

void loop() {

  // read the pushbuttons for setPoint value change:
  readButtons();

  // read the actual temperature (average from nSamples)
  sensorValue=readTemperature(nSamples);

  // time interval since last measurement
  actualTime = millis()/1000.0;
  dt = actualTime - lastTime;
  lastTime = actualTime;

  // error between setpoint and actual value
  error = setPoint - sensorValue;

  // error change since last measurement
  derror = error-lastError;
  lastError = error;

  // PID parameters
  P = error*Kp;
  I = I + error*dt*Ki;
  I=constrain(I, -255, 255);  // keep I values between -255 and 255
  D = derror/dt*Kd;

  // compute and send the Output value to PWM pin
  Out = P + I + D;
```

```
  Out = map(Out, 0, 255, 0, 255);
  Out = constrain(Out, 0, 255);
  analogWrite(outPin, int(Out));

  // update lcd with actual values
  lcdUpdate();

  // if arduino is reading 1 from serial port will send back the SensorValue
  if (Serial.read()=='1') Serial.println(sensorValue);

} //loop

// AUXILIARY FUNCTIONS
float readTemperature(int nS){
  float sV=0;
  for(int i=1; i<=nS; i++){
    sV = sV + ((analogRead(sensorPin)*LSBvalue)/AD595gain-b)/m;
    delay(2);
  }
  sV = sV/nS;
  return sV;
} //readTemperature

void readButtons(){
  // read button to increase setpoint
  buttonStateUp = digitalRead(buttonUpPin);
  if (buttonStateUp == HIGH) {
    setPoint = setPoint + 0.5;
   }
  // read button to decrease setpoint
  buttonStateDown = digitalRead(buttonDownPin);
  if (buttonStateDown == HIGH) {
    setPoint=setPoint-0.5;
  }
} //readButtons

void lcdUpdate(){
  lcd.clear();
  // first line
  lcd.setCursor(0, 0);
  lcd.print("SV=");   lcd.print(setPoint, 1);    // setpoint temperature
  lcd.print(" PV=");  lcd.print(sensorValue, 1); // actual temperature
  // second line
  lcd.setCursor(0, 1);
  if (lcdInfo==2){ //PID parameters
    lcd.print("P");   lcd.print(P,0);
    lcd.print(" I");  lcd.print(I,0);
    lcd.print(" D");  lcd.print(D,0);
  } else { //output parameters
      lcd.print("out:"); lcd.print(Out/255.0*100.0,1); lcd.print("% ");
      lcd.print(Out/255.0*Pmax,2); lcd.print("W");
    }

} //lcdUpdate
```

Matlab® software code

The Matlab® software used is as described:

```
function varargout = model3(varargin)
% MODEL3 MATLAB code for model3.fig
%      MODEL3, by itself, creates a new MODEL3 or raises the existing
%      singleton*.
%
%      H = MODEL3 returns the handle to a new MODEL3 or the handle to
%      the existing singleton*.
%
%      MODEL3('CALLBACK',hObject,eventData,handles,...) calls the local
%      function named CALLBACK in MODEL3.M with the given input arguments.
%
%      MODEL3('Property','Value',...) creates a new MODEL3 or raises the
%      existing singleton*.  Starting from the left, property value pairs
are
%      applied to the GUI before model3_OpeningFcn gets called.  An
%      unrecognized property name or invalid value makes property
application
%      stop.  All inputs are passed to model3_OpeningFcn via varargin.
%
%      *See GUI Options on GUIDE's Tools menu.  Choose "GUI allows only one
%      instance to run (singleton)".
%
% See also: GUIDE, GUIDATA, GUIHANDLES

% Edit the above text to modify the response to help model3

% Last Modified by GUIDE v2.5 28-Jun-2016 15:14:16

% Begin initialization code - DO NOT EDIT
gui_Singleton = 1;
gui_State = struct('gui_Name',       mfilename, ...
                   'gui_Singleton',  gui_Singleton, ...
                   'gui_OpeningFcn', @model3_OpeningFcn, ...
                   'gui_OutputFcn',  @model3_OutputFcn, ...
                   'gui_LayoutFcn',  [] , ...
                   'gui_Callback',   []);
if nargin && ischar(varargin{1})
    gui_State.gui_Callback = str2func(varargin{1});
end

if nargout
    [varargout{1:nargout}] = gui_mainfcn(gui_State, varargin{:});
else
    gui_mainfcn(gui_State, varargin{:});
end
% End initialization code - DO NOT EDIT


% --- Executes just before model3 is made visible.
function model3_OpeningFcn(hObject, eventdata, handles, varargin)
% This function has no output args, see OutputFcn.
% hObject    handle to figure
% eventdata  reserved - to be defined in a future version of MATLAB
% handles    structure with handles and user data (see GUIDATA)
% varargin   command line arguments to model3 (see VARARGIN)
```

```
% Choose default command line output for model3
handles.output = hObject;

trans = '00000000000000000000000000000000'; % 32x0
handles.out = trans;
a=getappdata(0, 'SerialPort');
b=getappdata(0, 'BRate');
handles.arduino = serial(a, 'BaudRate', b);
fopen(handles.arduino);


% Update handles structure
guidata(hObject, handles);

% UIWAIT makes model3 wait for user response (see UIRESUME)
% uiwait(handles.figure1);


% --- Outputs from this function are returned to the command line.
function varargout = model3_OutputFcn(hObject, eventdata, handles)
% varargout  cell array for returning output args (see VARARGOUT);
% hObject    handle to figure
% eventdata  reserved - to be defined in a future version of MATLAB
% handles    structure with handles and user data (see GUIDATA)

% Get default command line output from handles structure
varargout{1} = handles.output;



% --- Executes on button press in R1.
function R1_Callback(hObject, eventdata, handles)
% hObject    handle to R1 (see GCBO)
% eventdata  reserved - to be defined in a future version of MATLAB
% handles    structure with handles and user data (see GUIDATA)
if(strcmp(get(handles.R1, 'String'), 'OFF'))
        set(handles.R1, 'String', 'ON');
        set(handles.R1, 'Value', 1);
    else
        set(handles.R1, 'String', 'OFF');
        set(handles.R1, 'Value', 0);
end
handles.out(6) = int2str(get(hObject,'Value'));
%pause(0.00000000000000000000000000000001);
out=handles.out
fwrite(handles.arduino ,out);
guidata(hObject, handles);

% Hint: get(hObject,'Value') returns toggle state of R1



% --- Executes on button press in R2.
function R2_Callback(hObject, eventdata, handles)
% hObject    handle to R2 (see GCBO)
% eventdata  reserved - to be defined in a future version of MATLAB
% handles    structure with handles and user data (see GUIDATA)
```

```
if(strcmp(get(handles.R2, 'String'), 'OFF'))
        set(handles.R2, 'String', 'ON');
        set(handles.R2, 'Value', 1);
    else
        set(handles.R2, 'String', 'OFF');
        set(handles.R2, 'Value', 0);
end
handles.out(17) = int2str(get(hObject,'Value'));
out=handles.out
fwrite(handles.arduino ,out);
guidata(hObject, handles);
% Hint: get(hObject,'Value') returns toggle state of R2


% --- Executes on button press in R3.
function R3_Callback(hObject, eventdata, handles)
% hObject    handle to R3 (see GCBO)
% eventdata  reserved - to be defined in a future version of MATLAB
% handles    structure with handles and user data (see GUIDATA)
if(strcmp(get(handles.R3, 'String'), 'OFF'))
        set(handles.R3, 'String', 'ON');
        set(handles.R3, 'Value', 1);
    else
        set(handles.R3, 'String', 'OFF');
        set(handles.R3, 'Value', 0);
end
handles.out(20) = int2str(get(hObject,'Value'));
out=handles.out
fwrite(handles.arduino ,out);
guidata(hObject, handles);
% Hint: get(hObject,'Value') returns toggle state of R3


% --- Executes on button press in R4.
function R4_Callback(hObject, eventdata, handles)
% hObject    handle to R4 (see GCBO)
% eventdata  reserved - to be defined in a future version of MATLAB
% handles    structure with handles and user data (see GUIDATA)
if(strcmp(get(handles.R4, 'String'), 'OFF'))
        set(handles.R4, 'String', 'ON');
        set(handles.R4, 'Value', 1);
    else
        set(handles.R4, 'String', 'OFF');
        set(handles.R4, 'Value', 0);
end
handles.out(2) = int2str(get(hObject,'Value'));
out=handles.out
fwrite(handles.arduino ,out);
guidata(hObject, handles);
% Hint: get(hObject,'Value') returns toggle state of R4



% --- Executes on button press in E2.
function E2_Callback(hObject, eventdata, handles)
% hObject    handle to E2 (see GCBO)
% eventdata  reserved - to be defined in a future version of MATLAB
% handles    structure with handles and user data (see GUIDATA)

% Hint: get(hObject,'Value') returns toggle state of E2
```

```
if(strcmp(get(handles.E2, 'String'), 'OFF'))
        set(handles.E2, 'String', 'ON');
        set(handles.E2, 'Value', 1);
    else
        set(handles.E2, 'String', 'OFF');
        set(handles.E2, 'Value', 0);
end
handles.out(5) = int2str(get(hObject,'Value'));
out=handles.out
fwrite(handles.arduino ,out);
guidata(hObject, handles);



% --- Executes on button press in E3.
function E3_Callback(hObject, eventdata, handles)
% hObject    handle to E3 (see GCBO)
% eventdata  reserved - to be defined in a future version of MATLAB
% handles    structure with handles and user data (see GUIDATA)
if(strcmp(get(handles.E3, 'String'), 'OFF'))
        set(handles.E3, 'String', 'ON');
        set(handles.E3, 'Value', 1);
    else
        set(handles.E3, 'String', 'OFF');
        set(handles.E3, 'Value', 0);
end
handles.out(7) = int2str(get(hObject,'Value'));
out=handles.out
fwrite(handles.arduino ,out);
guidata(hObject, handles);
% Hint: get(hObject,'Value') returns toggle state of E3


% --- Executes on button press in E4.
function E4_Callback(hObject, eventdata, handles)
% hObject    handle to E4 (see GCBO)
% eventdata  reserved - to be defined in a future version of MATLAB
% handles    structure with handles and user data (see GUIDATA)
if(strcmp(get(handles.E4, 'String'), 'OFF'))
        set(handles.E4, 'String', 'ON');
        set(handles.E4, 'Value', 1);
    else
        set(handles.E4, 'String', 'OFF');
        set(handles.E4, 'Value', 0);
end
handles.out(8) = int2str(get(hObject,'Value'));
out=handles.out
fwrite(handles.arduino ,out);
guidata(hObject, handles);
% Hint: get(hObject,'Value') returns toggle state of E4


% --- Executes on button press in E5.
function E5_Callback(hObject, eventdata, handles)
% hObject    handle to E5 (see GCBO)
% eventdata  reserved - to be defined in a future version of MATLAB
% handles    structure with handles and user data (see GUIDATA)
if(strcmp(get(handles.E5, 'String'), 'OFF'))
        set(handles.E5, 'String', 'ON');
        set(handles.E5, 'Value', 1);
```

```
    else
        set(handles.E5, 'String', 'OFF');
        set(handles.E5, 'Value', 0);
end
handles.out(3) = int2str(get(hObject,'Value'));
out=handles.out
fwrite(handles.arduino ,out);
guidata(hObject, handles);
% Hint: get(hObject,'Value') returns toggle state of E5




% --- Executes on button press in E7.
function E7_Callback(hObject, eventdata, handles)
% hObject    handle to E7 (see GCBO)
% eventdata  reserved - to be defined in a future version of MATLAB
% handles    structure with handles and user data (see GUIDATA)
if(strcmp(get(handles.E7, 'String'), 'OFF'))
        set(handles.E7, 'String', 'ON');
        set(handles.E7, 'Value', 1);
    else
        set(handles.E7, 'String', 'OFF');
        set(handles.E7, 'Value', 0);
end
handles.out(18) = int2str(get(hObject,'Value'));
out=handles.out
fwrite(handles.arduino ,out);
guidata(hObject, handles);
% Hint: get(hObject,'Value') returns toggle state of E7


% --- Executes on button press in E8.
function E8_Callback(hObject, eventdata, handles)
% hObject    handle to E8 (see GCBO)
% eventdata  reserved - to be defined in a future version of MATLAB
% handles    structure with handles and user data (see GUIDATA)
if(strcmp(get(handles.E8, 'String'), 'OFF'))
        set(handles.E8, 'String', 'ON');
        set(handles.E8, 'Value', 1);
    else
        set(handles.E8, 'String', 'OFF');
        set(handles.E8, 'Value', 0);
end
handles.out(22) = int2str(get(hObject,'Value'));
out=handles.out
fwrite(handles.arduino ,out);
guidata(hObject, handles);% Hint: get(hObject,'Value') returns toggle state
of E8


% --- Executes on button press in E9.
function E9_Callback(hObject, eventdata, handles)
% hObject    handle to E9 (see GCBO)
% eventdata  reserved - to be defined in a future version of MATLAB
% handles    structure with handles and user data (see GUIDATA)
if(strcmp(get(handles.E9, 'String'), 'OFF'))
        set(handles.E9, 'String', 'ON');
```

```
        set(handles.E9, 'Value', 1);
    else
        set(handles.E9, 'String', 'OFF');
        set(handles.E9, 'Value', 0);
end
handles.out(21) = int2str(get(hObject,'Value'));
out=handles.out
fwrite(handles.arduino ,out);
guidata(hObject, handles);
% Hint: get(hObject,'Value') returns toggle state of E9


% --- Executes on button press in E10.
function E10_Callback(hObject, eventdata, handles)
% hObject    handle to E10 (see GCBO)
% eventdata  reserved - to be defined in a future version of MATLAB
% handles    structure with handles and user data (see GUIDATA)
if(strcmp(get(handles.E10, 'String'), 'OFF'))
        set(handles.E10, 'String', 'ON');
        set(handles.E10, 'Value', 1);
    else
        set(handles.E10, 'String', 'OFF');
        set(handles.E10, 'Value', 0);
end
handles.out(19) = int2str(get(hObject,'Value'));
out=handles.out
fwrite(handles.arduino ,out);
guidata(hObject, handles);
% Hint: get(hObject,'Value') returns toggle state of E10


% --- Executes on button press in E12.
function E12_Callback(hObject, eventdata, handles)
% hObject    handle to E12 (see GCBO)
% eventdata  reserved - to be defined in a future version of MATLAB
% handles    structure with handles and user data (see GUIDATA)
if(strcmp(get(handles.E12, 'String'), 'OFF'))
        set(handles.E12, 'String', 'ON');
        set(handles.E12, 'Value', 1);
    else
        set(handles.E12, 'String', 'OFF');
        set(handles.E12, 'Value', 0);
end
handles.out(4) = int2str(get(hObject,'Value'));
out=handles.out
fwrite(handles.arduino ,out);
guidata(hObject, handles);
% Hint: get(hObject,'Value') returns toggle state of E12


% --- Executes on button press in E13.
function E13_Callback(hObject, eventdata, handles)
% hObject    handle to E13 (see GCBO)
% eventdata  reserved - to be defined in a future version of MATLAB
% handles    structure with handles and user data (see GUIDATA)
if(strcmp(get(handles.E13, 'String'), 'OFF'))
        set(handles.E13, 'String', 'ON');
        set(handles.E13, 'Value', 1);
    else
        set(handles.E13, 'String', 'OFF');
```

```
        set(handles.E13, 'Value', 0);
end
handles.out(23) = int2str(get(hObject,'Value'));
out=handles.out
fwrite(handles.arduino ,out);
guidata(hObject, handles);
% Hint: get(hObject,'Value') returns toggle state of E13


% --- Executes on button press in E14.
function E14_Callback(hObject, eventdata, handles)
% hObject    handle to E14 (see GCBO)
% eventdata  reserved - to be defined in a future version of MATLAB
% handles    structure with handles and user data (see GUIDATA)
if(strcmp(get(handles.E14, 'String'), 'OFF'))
        set(handles.E14, 'String', 'ON');
        set(handles.E14, 'Value', 1);
    else
        set(handles.E14, 'String', 'OFF');
        set(handles.E14, 'Value', 0);
end
handles.out(24) = int2str(get(hObject,'Value'));
out=handles.out
fwrite(handles.arduino ,out);
guidata(hObject, handles);
% Hint: get(hObject,'Value') returns toggle state of E14


% --- Executes on button press in E15.
function E15_Callback(hObject, eventdata, handles)
% hObject    handle to E15 (see GCBO)
% eventdata  reserved - to be defined in a future version of MATLAB
% handles    structure with handles and user data (see GUIDATA)
if(strcmp(get(handles.E15, 'String'), 'OFF'))
        set(handles.E15, 'String', 'ON');
        set(handles.E15, 'Value', 1);
    else
        set(handles.E15, 'String', 'OFF');
        set(handles.E15, 'Value', 0);
end
handles.out(1) = int2str(get(hObject,'Value'));
out=handles.out
fwrite(handles.arduino ,out);
guidata(hObject, handles);
% Hint: get(hObject,'Value') returns toggle state of E15




% --- Executes when user attempts to close figure1.
function figure1_CloseRequestFcn(hObject, eventdata, handles)
% hObject    handle to figure1 (see GCBO)
% eventdata  reserved - to be defined in a future version of MATLAB
% handles    structure with handles and user data (see GUIDATA)

% Hint: delete(hObject) closes the figure
```

```
fclose(handles.arduino);
delete(instrfind('Name','Serial-COM3'));
delete(hObject);



% --- Executes during object creation, after setting all properties.
function time_CreateFcn(hObject, eventdata, handles)
% hObject    handle to time (see GCBO)
% eventdata  reserved - to be defined in a future version of MATLAB
% handles    empty - handles not created until after all CreateFcns called

% Hint: edit controls usually have a white background on Windows.
%       See ISPC and COMPUTER.
if ispc && isequal(get(hObject,'BackgroundColor'),
get(0,'defaultUicontrolBackgroundColor'))
    set(hObject,'BackgroundColor','white');
end



% --- Executes during object creation, after setting all properties.
function image_CreateFcn(hObject, eventdata, handles)
% hObject    handle to image (see GCBO)
% eventdata  reserved - to be defined in a future version of MATLAB
% handles    empty - handles not created until after all CreateFcns called

% Hint: place code in OpeningFcn to populate image



% --- Executes on mouse press over axes background.
function image_ButtonDownFcn(hObject, eventdata, handles)
% hObject    handle to image (see GCBO)
% eventdata  reserved - to be defined in a future version of MATLAB
% handles    structure with handles and user data (see GUIDATA)
```